Heliyon 9 (2023) e18371

Contents lists available at ScienceDirect

Heliyon

journal homepage: www.cell.com/heliyon

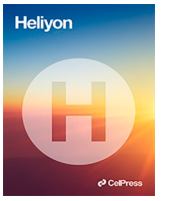

Modeling assessment of groundwater vulnerability to contamination risk in a typical basement terrain using TOPSIS-entropy developed vulnerability data mining technique

Olanrewaju Fred Atenidegbe [a,b,*], Kehinde Anthony Mogaji [a]

[a] Department of Applied Geophysics, Federal University of Technology, Akure, Nigeria
[b] Computing Science and Mathematics, University of Stirling, Stirling FK9 4LA, United Kingdom

ARTICLE INFO

Keywords:
Groundwater vulnerability
Geophysics
Remote sensing and GIS
TOPSIS
Entropy
Python programming

ABSTRACT

This study involved a comparative analysis in the groundwater vulnerability domain, which is a crucial component of groundwater management decision support systems (DSS). This was achieved by creating models that covered the range of algorithms from the subjective to the data-driven. The study was conducted in a basement complex area. Databases of climatic, remote sensing, and geophysical datasets were created using varieties of data acquisition techniques. The datasets included in this assessment were: rainfall (R), land use (LU), bedrock topography (BT), recharge rate (Re), and slope (S). The slope and rainfall were determined to have the highest (0.78) and lowest (0.01) weighted factors, respectively, using the entropy method. For the development of the TOPSIS-Entropy model algorithm, the weights results were combined with the TOPSIS outranking method. To generate the Groundwater Vulnerability Model map of the study area, the hybrid model was applied to griddled raster layers of the factors. Also, the TOPSIS and Entropy-WLA model algorithms were also explored and used to generate groundwater vulnerability maps. The TOPSIS-Entropy algorithms produced an accuracy of 70%, while TOPSIS and Entropy-WLA produced accuracy of 50 and 47%, respectively. The resulting model maps were validated by using correlation technique on the produced map and the longitudinal conductance map of the study area. The TOPSIS-Entropy, which followed an object-oriented model pattern, demonstrates greater accuracy and has the potential to provide appropriate insights and alternatives to decision-making in the field of groundwater hydrology in the study area and other regions of the world with comparable geology.

1. Introduction

Because it makes up roughly 95% of the freshwater in the earth's systems, groundwater is one of the most significant natural resources that are essential to human sustenance in our environment [1,2]. In the majority of the world, this resource—which is frequently found in pore spaces and weak zones in the earth's subsurface—is the primary source of water for domestic uses and accounts for about 40% of the water used for irrigation and industrial purposes. In order to enable the availability of portable water, it is therefore essential to explore significant groundwater quantity and quality [3]. The quality of groundwater is a major factor that must be taken into account for the proper location of a well or borehole despite the possibilities of exploring an economically sufficient

* Corresponding author. Department of Applied Geophysics, Federal University of Technology, Akure, Nigeria.
E-mail address: ola00229@students.stir.ac.uk (O.F. Atenidegbe).

https://doi.org/10.1016/j.heliyon.2023.e18371
Received 17 January 2023; Received in revised form 13 July 2023; Accepted 14 July 2023
Available online 18 July 2023

quantity of groundwater. This thorough investigation shows the degree of groundwater portability, which is primarily influenced by the rapid growth in the human population and the consistent anthropogenic activities that accompany the growth. As a result, there has been an ongoing need to investigate cutting-edge techniques to determine vulnerability. According to the studies [4,5], groundwater vulnerability refers to an aquifer unit's susceptibility to pollution, leachate plumes brought on by anthropogenic activities, and pollutant properties from the surface. According to a study [6], an area's groundwater vulnerability can be evaluated using a variety of conditioning factors. According to studies [4,7–9], these variables, such as land use, net recharge, longitudinal conductance, aquifer properties, topography, and hydraulic conductivity, among others, can provide information about how vulnerable an area may be.

For assessing groundwater vulnerability, a variety of existing techniques have been employed, including process simulation,

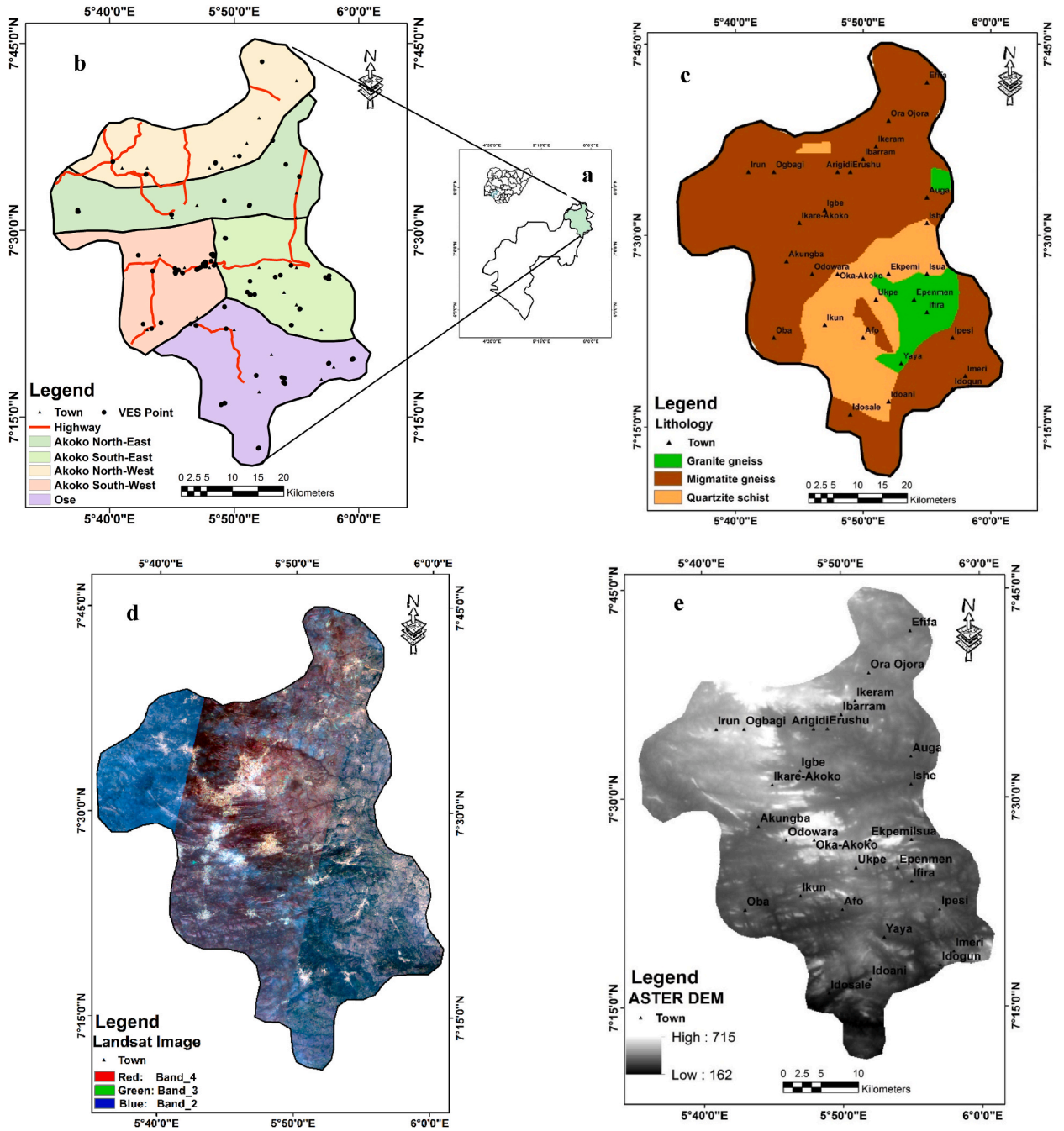

Fig. 1. Location maps showing a) map of Ondo State and Nigeria and b) study area map displaying the data acquisition points c) geologic map of the study area (Modified after NGSA, 2006) d) Landsat image of the study area e) ASTER DEM of the study area.

overlay/index techniques, and statistical methods [7,10]. Due to its inherent sensitivity analysis of the various parameters present, the DRASTIC index model of the overlay index method is the one most frequently used to assess groundwater vulnerability [4,11]. This model is often developed in conjunction with a spatial tool via a geographic information system (GIS) to create a GIS-based DRASTIC model and a groundwater vulnerability index that successfully assesses vulnerability over time. The Analytical Hierarchy Process (AHP) is one of the multi-criteria decision methods (MCDM) that the model has integrated internally to produce better performance [12,13]. AHP and weight linear average (WLA) techniques, which compute the weights of the DRASTIC model parameters and rank the alternatives, have been shown to be applicable and to have a high degree of accuracy when validated using qualitative and quantitative means [10]. The subjectivity and bias of the model as a result of the expert knowledge required to drive the model, however, is one of the major drawbacks of the weighting and ranking techniques prominent in previous works [14]. In order to compare models with inherent object orientation to other types of models and to develop a robust MCDM ranking technique for various groundwater vulnerability conditioning factors, this research compares them.

One of the methods of MCDM for solving problems is the technique for order preference by similarity to the ideal solution (TOPSIS). It works by selecting the best alternative among various variables (alternatives) using the idea of the compromise solution. The studies [15–17] made the initial proposal. Because of the TOPSIS method's clarity, logic, and understandable conceptual structure, it has been widely used in literature. Additionally, it is logically sound and intuitive, reflecting how people make decisions. Also, it is simple to compute with good computational efficiency [18]. Weights of criteria must be predetermined before the TOPSIS algorithm is used; these weights may be either subjective or objective. This will help to evaluate alternatives and, as a result, allow the TOPSIS algorithm to determine the best alternatives [17]. Examples of subjective weighting methods include direct rating, ranking method, point

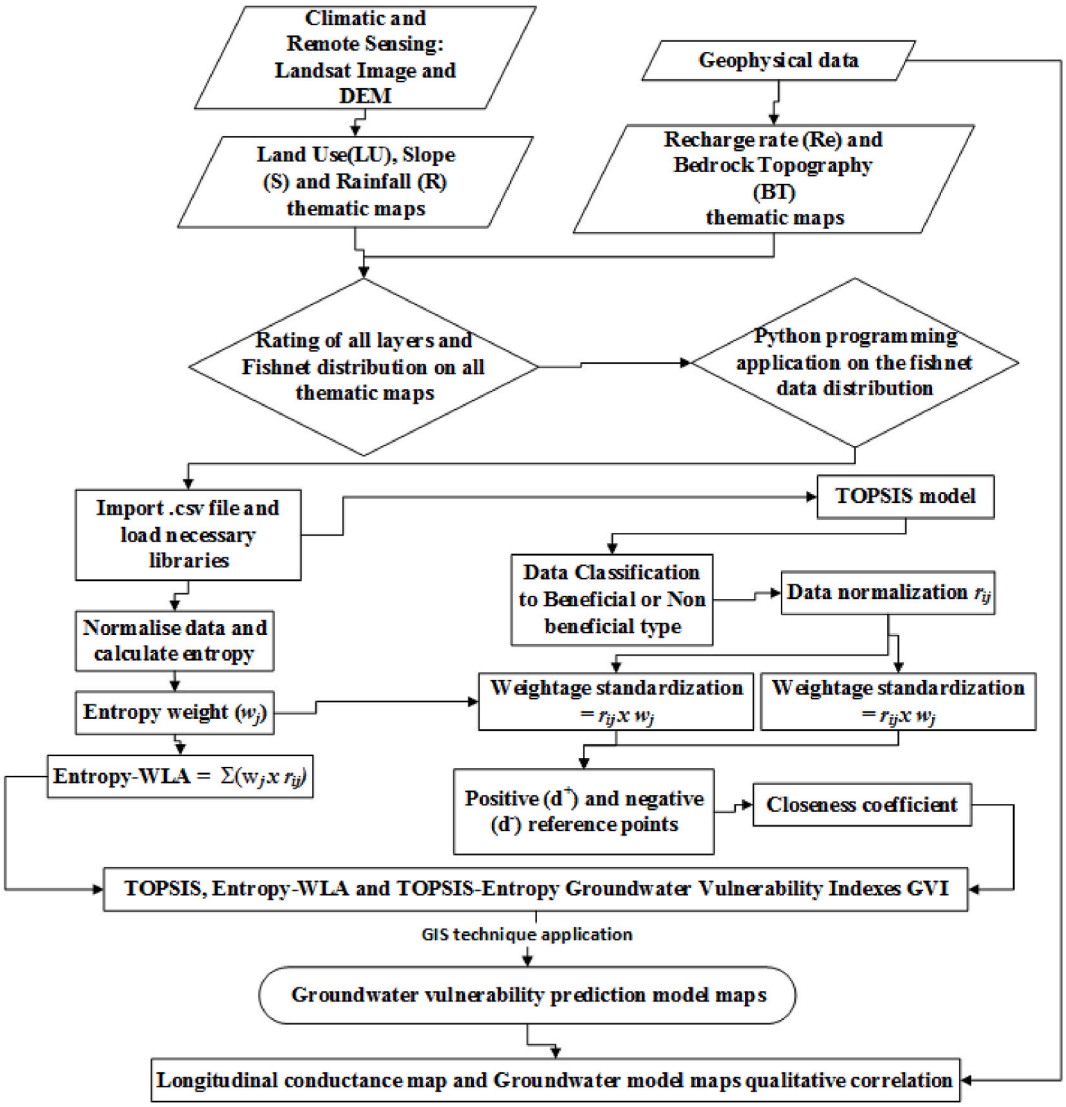

Fig. 2. Flowchart of the Methodology for the vulnerability assessment.

allocation, pairwise comparison (used within the method of AHP), swing method, and Delphi method. Decision makers are given priority to assign importance to criteria at their own preferences. In objective weighting methods, weights are calculated using mathematical techniques, and decisions regarding the relative importance of criteria are not left up to experts or decision-makers. Entropy, CRITIC, a literature review, the standard deviation, or a statistical variance procedure are some examples [17]. Shanon first put forth the entropy method of weight determination in 1948, which Rudolph Clausius had derived from thermodynamics in 1865 [19]. By calculating the entropy and entropy weight, it is possible to determine the weight values of individual parameters in a decision-making process [20]. In contrast to other popular MCDAs, the entropy method only requires the creation of an evaluation matrix [20]. Expert judgement is not necessary. The entropy method has been used extensively in the literature, for instance in the military to evaluate weapon systems and in conjunction with other MCDA methods to facilitate efficient decision-making [19,21]. In order to create an objective TOPSIS modeling algorithm that is more reliable than other algorithms, the distinct objective attributes of the entropy model will be investigated. Three different models will be compared and evaluated in this study. Entropy-WLA, TOPSIS-Entropy, and TOPSIS models will be used. The goals are to (1) create three subjectivities-varying models. (2) produce thematic layers for each model, and (3) use correlation analysis to verify the findings. In order to reduce the computational cost of the computing algorithms, the Python programming language will also be used. This is a result of Python's specialization in exploratory data analysis and the availability of strong libraries to quickly and accurately compute the algorithm [22].

2. Study area description

The study area is 1492.55 square kilometres in size and is geographically situated in the southwest of Nigeria (Fig. 1a). Five local government areas make up the study area (Fig. 1b): Ose, Akoko South-west, Akoko South-east, Akoko North-west, and Akoko North-east. The region is located between latitudes 7°10′0″ and 7°45′0″ north and 5°30′0″ and 6°0′0″ east. According to the study [23], the study area has highly undulating topography that tends to rise as high as 1500 m above sea level. The region has a hot and humid climate that is typically influenced by winds from the Sahara Desert. Around August to October is when the region's rainy season peaks, with annual precipitation averaging between 1500 and 2000 mm. The average annual temperature ranges between 26 and 28 °C with a mean relative humidity range of 75–95% [24].

The study area is a part of Nigeria's basement Precambrian complex. Due to the basement complex's hilly terrain, extremely high runoff rates, and low infiltration rates, crystalline rocks dominate the landscape [23]. Additionally, the crystalline rocks have low porosity and permeability to fluid percolation, which is primarily due to the properties of the underlying rock units and the lack of secondary porosity, which results in a generally low and irregular groundwater occurrence [4,23]. The study area's aquifer is known to be either a weathered layer or a fractured basement. Low percolation results in minimal groundwater existence and low yield [25,26]. In the study area, the groundwater is concentrated in small, isolated basins and pockets.

The basement complex rocks of the southwestern part of Nigeria underlie the study area's geologic setting [27]. Granite, Migmatite-gneiss, and Quartzite are among the recognized rock units in the region. More than 70% of the area is underlain by Migmatite–gneiss. The geologic map was extracted from the scanned copy of the regional and mineral resources map of Ondo State [28]. The geologic map of the region is shown in Fig. 1c.

3. Materials and methodology

This study used surface and subsurface datasets that included climatic, remote sensing, and geophysical information. There are four phases to the methodology's execution (see Fig. 2). The first stage involved gathering the climatic, remote sensing, and geophysically based parameters as well as their processing and interpretation. Additionally, the groundwater vulnerability assessment of the study used ArcGIS software to spatially generate thematic maps of the conditioning factors taken into account. Following that, spatial fishnet points with equal spacing were placed on each map to extract pixel values for the computation of the TOPSIS-Entropy groundwater vulnerability index. This index was then synthesized in the ArcGIS environment to create the groundwater vulnerability model map of the study area. Finally, a longitudinal conductance map of the study area was used to validate the proposed model. The flowchart methodology used for the study is shown in Fig. 2.

3.1. Climatic data

The rainfall data from the study's climate are significant because they can be used to assess an area's groundwater vulnerability as well as its potential. The annual average volume of water that permeates the vadose zone and gets to the water table is represented by the rainfall, R (net recharge) [29]. With increased rainfall or net recharge, an aquiferous zone's vulnerability status rises. The climatic information used for this study in the study area was the data on average rainfall. The data source is the European Centre for

Table 1
Information on the sources of the raster data used.

Types of Data	Data details	Format	Layers extracted	Layers generated
Remote Sensing	Landsat 8	TIFF	Land Use	Land Use
Rainfall data	ERA-Interim	Excel	Distribution	Rainfall distribution
ASTER DEM	DEM	TIFF	Slope	Slope

Medium-Range Weather Forecasting (ERA-Interim), which is shown in Table 1. A recent global atmospheric reanalysis (third-generation reanalysis) with improved temporal and spatial resolution is the European Centre for Medium-Range Weather Forecasting (ECMWF) Reanalysis-Interim (ERA-Interim). The ECWMF datasets, which cover the years 1979 through the present, have a spatial resolution of 0.125° latitude by 0.125° longitude (spectral truncation T159).

3.2. Remote sensing data

In this study, the Land Use (LU) of the study area was extracted from the LANDSAT 8 image of the study area (Fig. 1d). In the year 2020, this image was downloaded from Earth Explorer with path 189 and row 055. According to the studies [30,31], one hydrogeological feature that affects an area's rate of infiltration, runoff, and evapotranspiration is LU. The relationship between LU and groundwater quality has been documented in the literature [23,32,33]. These studies covered how the area's prevalent LU practices severely restrict groundwater recharge in their study areas, affecting the groundwater's vulnerability. For instance, it is uncommon for fluid or contaminants to percolate beneath the surface in rock-occupied areas. However, the aquifer unit beneath populated or vegetated areas will be more vulnerable to pollution as a result of human activity and surface fluid discharge. Water bodies, cultivated areas, bare ground, outcrops, built-up areas, vegetated areas, and other LU classes may be present in a study region. Because of the high infiltration rate in these areas compared to built-up and outcrop areas, which will experience high runoff and low infiltration, they are good zones for groundwater recharge.

Additionally, the slope map was created using the slope analysis tool in the ArcGIS 10.3 software program from the Aster Digital Elevation Map (DEM) of the study area (Table 1 and Fig. 1e). The slope percent indicates the amount of surface runoff, which varies from one location to another. Because areas with low slope percent will have a low probability of runoff and its pollutants being retained long enough to infiltrate it, and vice versa for areas with high slope percent, this degree has an impact on the vulnerability from one place to another [3].

Table 2
Summary of the interpreted primary geoelectric parameters.

VES	Layer resistivity (Ωm)					Layer thickness (m)				Curve Type
	ρ_1	ρ_2	ρ_3	ρ_4	ρ_5	h_1	h_2	h_3	h_4	
1	456	90	1476			1.2	1.2			H
2	942	26	704			0.8	0.7			H
3	603	145	21,196			0.8	3			H
4	2377	139	6065			0.4	6.2			H
5	1522	229	10,615			1	14.8			H
6	1461	140	1429			0.7	2.8			H
7	1076	122	3124			0.7	2.4			H
8	426	122	658			0.3	5.4			H
9	1399	215	2322			0.9	1.9			H
10	878	155	2692			2.5	13.8			H
11	279	18	2557			0.7	0.4			H
12	4516	91	16,224			1.2	12.2			H
13	4721	343	268	1191		1.3	0.4	14.3		QH
14	2060	357	5670			1.2	14.2			H
15	1208	171	3917			3.3	69			H
16	2277	480	1195	295	20,096	1.1	1.5	6.1	10.6	HKH
17	525	77	2563			2	6.5			H
18	23	109	533			1	7.5			A
19	566	45	791	105	19,560	0.5	0.5	4.5	15	HKH
20	101	254	137	6265		1.2	2.8	28		KH
21	53	130	80	203		1.1	2.9	5.4		KH
22	210	25	301	131	859	0.7	0.3	3.4	6.1	HKH
23	354	131	609			1.8	4.3			H
24	181	70	3633			1.1	1.6			H
25	147	309	20,728			1.4	5.6			A
?	?					?				?
?	?					?				?
110	63	121	25	6776		0.8	1.6	3.4		KH
111	32	88	549			0.9	5			A
112	85	39	3523			1	2.6			H
113	64	30	2490			1.5	3.2			H
114	281	86	148	18,315		0.6	1.1	4.4		HA
115	132	83	7708			0.8	3.2			H
116	255	641	192	15,396		0.9	1.6	2.7		KH
117	404	71	1304			1	4			H
118	171	92	18,785			1.6	3			H

3.3. Geophysical data

3.3.1. 1D depth sounding data acquisition, processing, and interpretation

One hundred and eighteen (118) VES data using half-electrode spacing (AB/2) were acquired across the study area using the Vertical Electrical Sounding (VES) technique of the Electrical Resistivity (ER) method (Fig. 1b). This method makes use of self-induced current that is discharged into the ground through pairs of electrodes (current electrodes), while a different pair of electrodes (potential electrodes) measures the potential created.

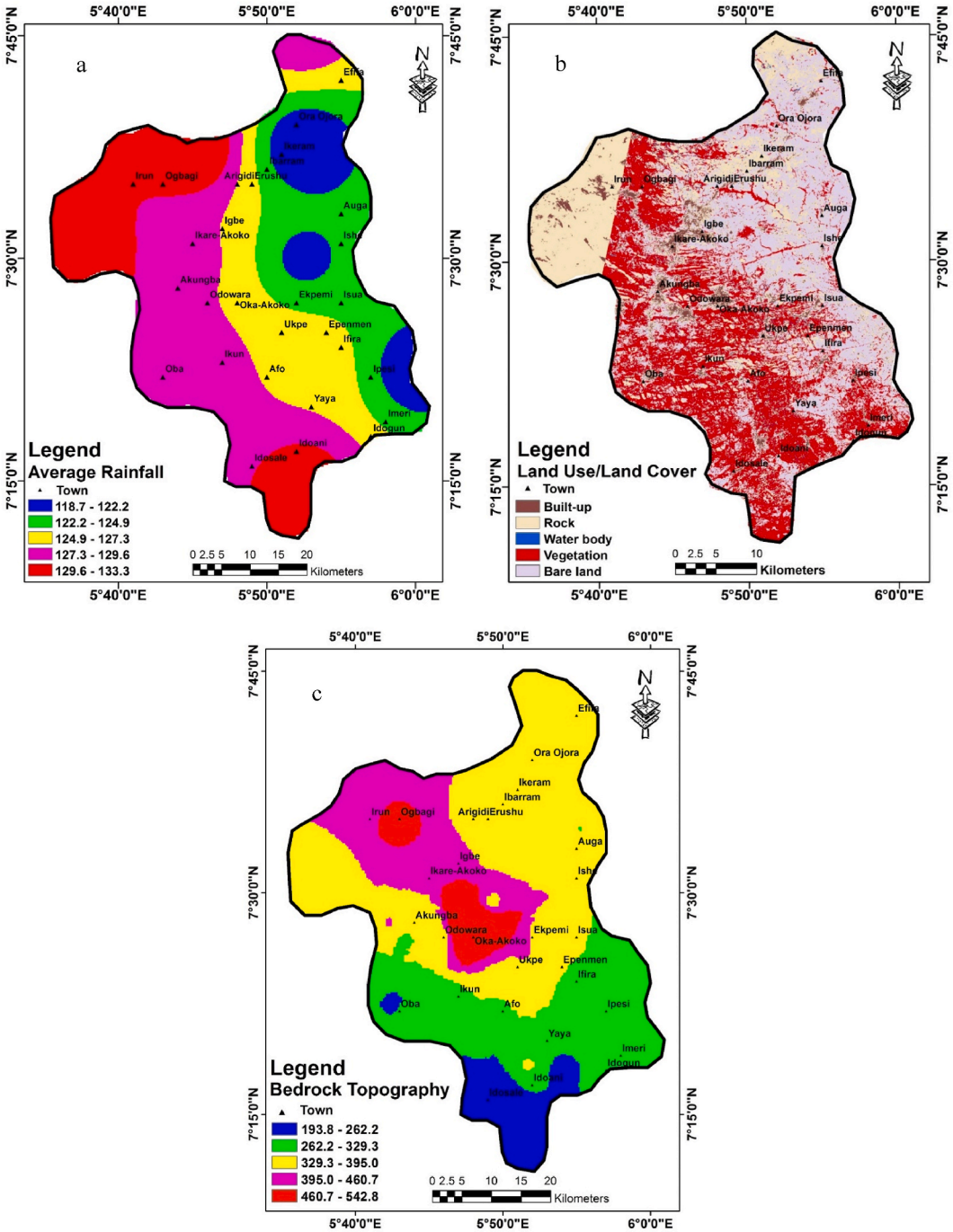

Fig. 3. The thematic layers produced for the applied data-driven TOPSIS-Entropy model (a) Rainfall (R); (b) Land use (LU); (c) Bedrock Topography (BT).

Due to its speed and relatively high depth of investigation, the Schlumberger array was preferred in this situation [34]. The apparent resistivity was plotted against the half-current electrode spacing (AB/2) on a log-log graph, which produced a resistivity curve for each VES point. The layer resistivity and thickness were computed using these curves after additional processing to determine the primary geoelectric parameters. These parameters were loaded into the WinResistTM software along with the field data to carry out an inversion procedure [35]. Table 2 and Fig. 3 show examples of resistivity curves and a summary of the primary geoelectric parameters, respectively.

3.3.2. Derived secondary geoelectric parameters

The primary geoelectric parameters shown in Table 2 were used to compute the secondary geoelectric parameters, Table 3, which were used in this study. As shown in equations (1)–(3), they include bedrock topography (BT), recharge rate (Re), and longitudinal conductance (Lc).

$$BT = Elevation\ (m) - Depth\ to\ bedrock\ (m) \quad (1)$$

$$Re = 34.41log10\ (\rho) + 1.05\ (D) + 128.38 \quad (2)$$

$$Lc = h_n/\rho_n = h_1/\rho_1 + h_2/\rho_2 + \ldots. + h_n/\rho_n \quad (3)$$

where n = number of layers overlying the aquifer unit, h = layer thickness, D = depth to top of aquifer, ρ = unsaturated layer resistivity.

3.3.3. Objective model preparation

3.3.3.1. Preparation of groundwater vulnerability conditioning factors thematic layers. In order to assess the vulnerability of an aquifer unit, this study took into account five (5) groundwater vulnerability conditioning factors. The following variables are taken into consideration: rainfall (R), land use (LU), bedrock topography (BT), recharge rate (Re), and slope (S). The factor's thematic layers were

Table 3
Summary of the derived secondary geoelectric parameters.

VES	Lat	Long	E (m)	BT (m)	Re (mm/year)	Lc (mhos)
1	7.3726	5.782	299.872	297.472	221.135	0.002632
2	7.3724	5.7825	300.64	299.14	231.5571	0.000849
3	7.4453	5.7239	329.774	325.974	224.8907	0.001327
4	7.4452	5.72416	330.69	324.09	244.9692	0.000168
5	7.44521	5.72424	331.305	315.505	238.9369	0.000657
6	7.37594	5.73524	267.587	264.087	238.0106	0.000479
7	7.37552	5.73532	269.496	266.396	233.4397	0.000651
8	7.58986	5.8083	360.208	354.508	219.173	0.000704
9	7.59042	5.808326	361.53	358.73	237.5726	0.000643
10	7.59928	5.840215	371.181	354.881	232.2906	0.002847
11	7.588169	5.902494	356.228	355.128	213.2682	0.002509
12	7.619999	5.884966	395.119	381.719	255.4001	0.000266
13	7.725406	5.87069	410.547	394.547	247.2782	0.001442
14	7.725434	5.87069	410.608	395.208	243.6702	0.000583
15	7.374188	5.7116	296.41	224.11	261.4374	0.003338
16	7.37413	5.711435	293.486	274.186	237.8989	0.002732
17	7.37452	5.775158	337.124	328.624	244.8637	0.008713
18	7.57175	5.92052	381.352	372.852	224.0807	0.00381
19	7.539312	5.820104	452.453	431.953	176.2871	0.043478
20	7.52084	5.749325	455.089	423.089	226.0169	0.017684
21	7.520675	5.74963	455.393	445.993	209.9749	0.022905
22	7.5207	5.74966	346.191	335.691	200.0725	0.043062
23	7.304917	5.86299	350.029	343.929	210.4928	0.026629
24	7.305333	5.86291	353.851	351.151	217.9812	0.005085
25	7.396825	5.82033	354.201	347.201	207.2217	0.006077
?	?	?	?	?	?	?
?	?	?	?	?	?	?
110	7.26853	5.820464	349.632	343.832	198.4739	0.025922
111	7.26834	5.82108	337.584	331.684	181.1172	0.028125
112	7.326942	5.992162	504.745	501.145	195.8213	0.011765
113	7.326692	5.99169	503.072	498.372	192.1057	0.023438
114	7.326637	5.99108	370.79	364.69	208.0567	0.014926
115	7.3278	5.9926	372.724	368.724	202.1889	0.006061
116	7.327165	5.992634	361.187	355.987	222.2355	0.006026
117	7.574587	5.71538	342.351	337.351	219.1156	0.002475
118	7.574559	5.715157	341.94	337.34	206.8974	0.009357

E: Elevation; BT: Bedrock topography; Re: Recharge rate; Lc: Longitudinal conductance.

produced using the ArcGIS 10.3 software. The generated layers are displayed in Figs. 3a–c and 4a–b; they were produced using the inverse distance weighting (IDW) technique. In order to extract pixel values from the points for purposes of robust computation, evenly spaced fishnet points (see Fig. 5) were posted on the thematic layers. The algorithm for the Python-based TOPSIS-Entropy model used the extracted values as one of its inputs. Table 4 displays the values of the extracted pixels.

3.3.3.2. The TOPSIS index theory. One of the MCDMs introduced by Ref. [15] is this approach. It hinges on the idea that the selected alternative should be the furthest from the negative ideal solution and the closest to the positive ideal solution in Euclidean space [36]. The positive ideal solution, which comprises the satisfying solutions, is a hypothetical situation in which all attribute values correspond to the maximum attribute values in the database, whereas the negative ideal solution happens when all attribute values correspond to the minimum attribute values in the database [37]. Thus, TOPSIS provides a solution that is not only the furthest from the hypothetically worst but also the closest to the hypothetically best.

TOPSIS was first proposed by Hwang and Yoon [15] and Li [16]. A decision matrix (D_{ij}) is first constructed as shown in equ 4 below:

$$D = D_{ij} = (D_{11}\ D_{12}\ldots\ldots D_{1n}\ D_{2n}\ D_{2n}\ldots\ldots D_{2n}\ D_{m1}\ D_{m2}\ldots D_{mn}) \tag{4}$$

for $i = 1,2\ \ldots,m;\ j = 1,2,\ \ldots,n$

Where, D_{im} = feasible alternatives, D_{jn} = evaluation criteria, m = number of alternative and n = number of criteria.

Then, using Equation (5) below, the standardized matrix is calculated by eliminating the complex relations and anomalies from the decision matrix.

$$r_{ij} = \frac{D_{ij}}{\sqrt{\sum_{i=1}^{m} D_{ij}^2}} \quad i = 1,2...m;\ j = 1,2,...n \tag{5}$$

The next step is to use Equation (6) below to calculate the weighted standardized matrix $F = (f_{ij})_{m\ x\ n}$. Note that depending on preference, either objective or subjective methods may be used to determine the weights of the criteria (w_j).

$$f_{ij} r_{ij} \times w_j \tag{6}$$

After that, the positive (A) and the negative (E) ideal reference points are determined (as in equations (7) and (8) below formed from equ 9). First,

$$\text{let } f_j^+ = \max\{f_{1j}, f_{2j}\ \ldots f_{mj}\} \text{ and } f_j^- = \min\{f_{1j}, f_{2j}\ \ldots f_{mj}\}\ (j = 1,2,\ \ldots n) \tag{7}$$

$$\text{therefore, the positive reference point } A = \{\ f_1^+, f_2^+\ \ldots f_n^+\} \tag{8}$$

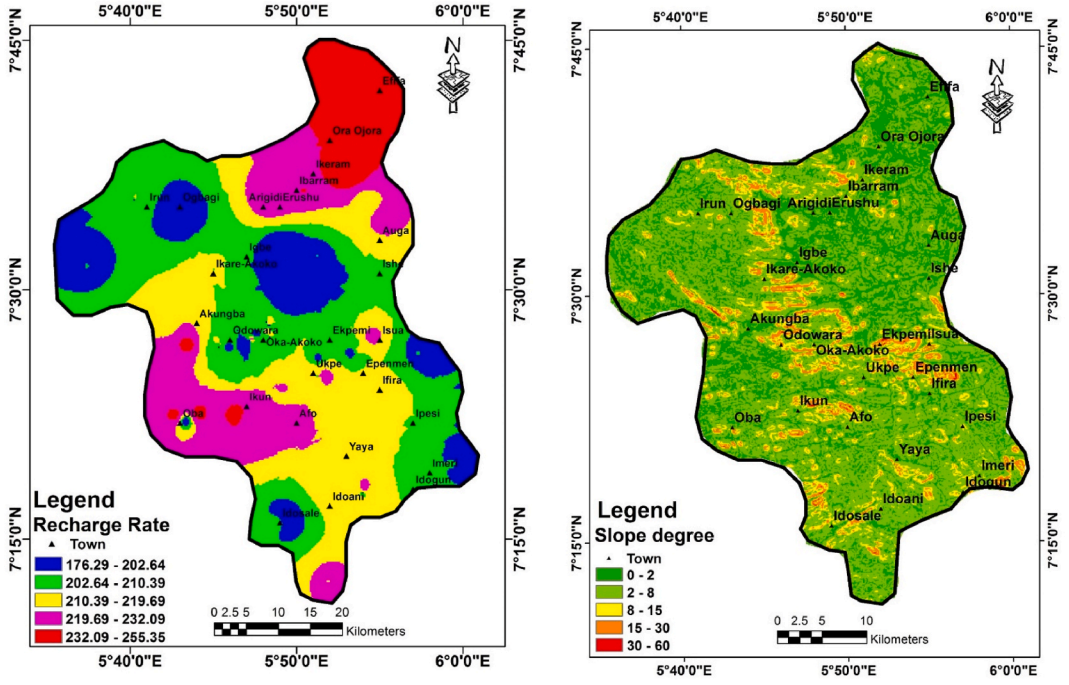

Fig. 4. The thematic layers produced for the applied data-driven TOPSIS-Entropy model (a) Recharge rate (Re); (b) Slope (S).

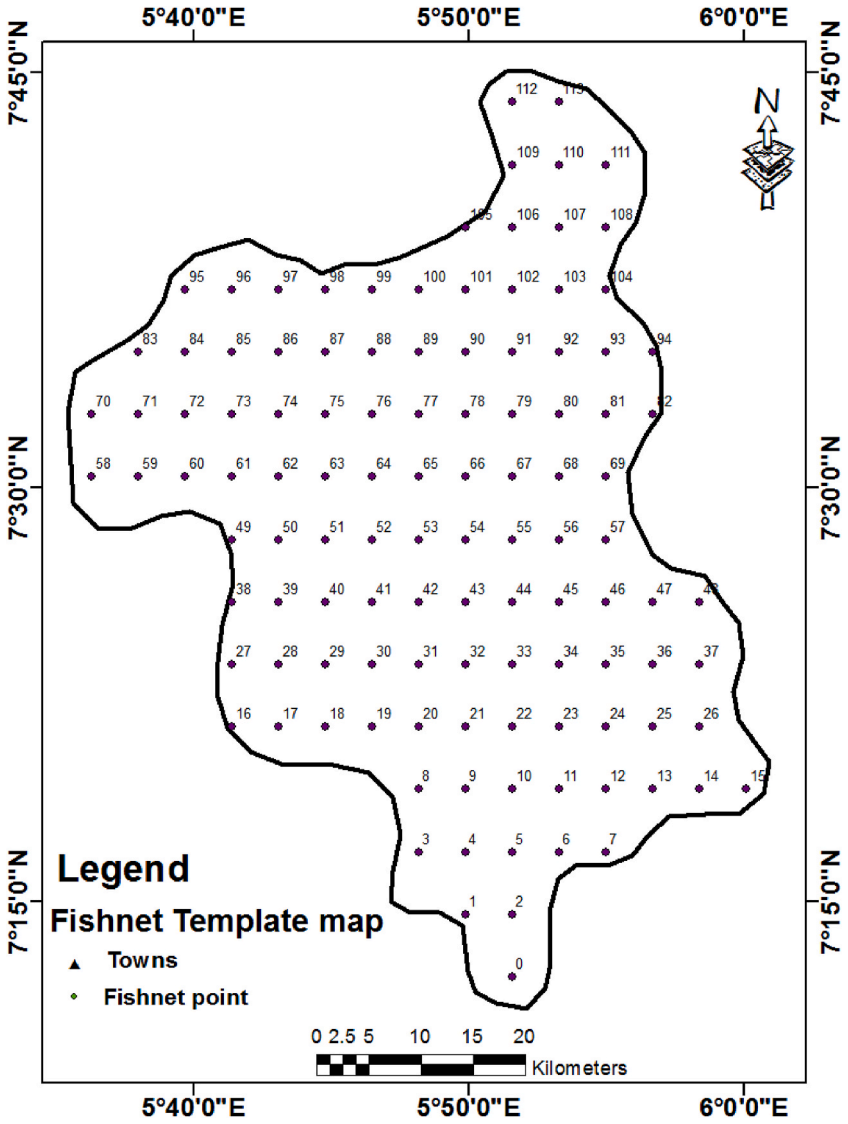

Fig. 5. Fishnet template map of the study area.

and the negative reference point $E = \{ f_1, f_2 \ldots f_n^- \}$ (9)

The distances to the ideal positive and negative reference points are calculated in the following step. The following equations (10) and (11) can be used to calculate them.

$$d^+ = \sqrt{\sum_{j=1}^{n} \left[f_{ij} - (f_{ij})_a \right]^2} \tag{10}$$

$$d^- = \sqrt{\sum_{j=1}^{n} \left[f_{ij} - (f_{ij})_e \right]^2} \tag{11}$$

where $(f_{ij})_A$ and $(f_{ij})_E$ are the values in the positive and negative ideal reference points respectively., d+ and d− are the distances to the positive and negative ideal reference points, respectively.

The final step involves calculating the closeness coefficient from the ideal solution and ranking the alternatives in descending order with equation (12) below.

Table 4
Decision matrix for the groundwater vulnerability conditioning factors.

Fishnet no	Longitude	Latitude	R	LU	BT	Re	S
0	5.859741	7.204569	130.3	38.6	205.6	222.2	3.6
1	5.831421	7.242249	130.3	35.3	212.6	205.3	4.2
2	5.859741	7.242249	131.3	35.3	227.9	212.7	12.1
3	5.803101	7.279928	128.8	32.4	205.8	203	12
4	5.831421	7.279928	129.5	29.7	212.1	199.7	7.2
5	5.859741	7.279928	130.3	27.6	267.6	211.2	3.7
6	5.888062	7.279928	130.3	32.2	259.9	214	3.8
7	5.916382	7.279928	129	30.1	260.5	214.4	4.3
8	5.803101	7.317607	128.2	32.4	267.6	215.2	10
9	5.831421	7.317607	128.1	28.8	271.4	212.4	5.3
10	5.859741	7.317607	128	32.7	317.5	214.2	5.8
11	5.888062	7.317607	127.7	32.2	268.7	217.1	11.8
12	5.916382	7.317607	127	27	265.8	215.6	11.6
13	5.944702	7.317607	125.6	25.1	280.1	206	9.6
14	5.973022	7.317607	124	29	292.7	203.8	1.2
15	6.001343	7.317607	122.9	25.6	308.6	201.2	2.4
16	5.689819	7.355286	128.7	21	277.5	224.7	0.6
17	5.71814	7.355286	128.8	19.3	280.7	216.3	2.1
18	5.74646	7.355286	128.9	26.1	283.5	226.6	3.3
19	5.77478	7.355286	128.7	30	294.1	229.5	2.8
20	5.803101	7.355286	128	30	306.4	226.3	4.5
21	5.831421	7.355286	127.4	30	311	224	2.2
22	5.859741	7.355286	127.1	35.6	326.5	219.2	1.8
23	5.888062	7.355286	127	27.5	299.8	216.7	7.8
24	5.916382	7.355286	126.2	23.8	301.5	214.8	5.4
25	5.944702	7.355286	124.2	26.8	296.1	209.7	10.2
26	5.973022	7.355286	121.8	26.5	301.7	204.1	2
27	5.689819	7.392965	128.8	25.1	287.2	224	1.3
28	5.71814	7.392965	128.8	26.6	275.4	226.2	2.5
29	5.74646	7.392965	128.9	27.1	288.6	224.1	4.3
30	5.77478	7.392965	128.6	24.9	301.2	226.4	7.5
31	5.803101	7.392965	127.7	25.4	343.7	219.9	17.6
32	5.831421	7.392965	127	22.4	348.4	218.9	3.6
33	5.859741	7.392965	126.9	23.1	353.6	217.4	5.9
34	5.888062	7.392965	126.8	20.8	335.8	214.7	3.7
35	5.916382	7.392965	125.8	19.5	301.3	216.4	1
36	5.944702	7.392965	123.8	19.1	305.1	211.8	1.9
37	5.973022	7.392965	121.6	20.7	304.2	205.3	5.9
38	5.689819	7.430644	128.9	26.8	327.8	223	0.9
39	5.71814	7.430644	128.5	23.6	328.2	226.8	2.1
40	5.74646	7.430644	128.2	17.7	347	208.9	1.2
41	5.77478	7.430644	127.7	20.6	405.6	204.1	5.4
42	5.803101	7.430644	127	31.2	513	205.2	6.7
43	5.831421	7.430644	126.2	31.2	415.4	212.9	6.1
44	5.859741	7.430644	125.6	23	413.7	204.8	10.7
45	5.888062	7.430644	125.3	18.9	361.1	203.6	7.9
46	5.916382	7.430644	124.8	25.4	336.2	210.8	2.2
47	5.944702	7.430644	124	19.7	308.9	202.8	0.3
48	5.973022	7.430644	123.1	13.2	303.4	199.5	3.4
49	5.689819	7.468323	129.3	25.6	372.4	215.7	3
50	5.71814	7.468323	128.3	24.7	360.1	218.5	4.5
51	5.74646	7.468323	127.9	18.8	354.6	210.6	0.7
52	5.77478	7.468323	127.5	30.1	495.3	203	26.7
53	5.803101	7.468323	126.5	20.9	542.9	198.1	0.8
54	5.831421	7.468323	124.8	26.1	493.9	205.4	7.2
55	5.859741	7.468323	123.2	19.5	403.3	207.7	1.9
56	5.888062	7.468323	122.9	19.5	360.8	209.4	5.2
57	5.916382	7.468323	123.5	18.1	343.9	215.2	7.3
58	5.604858	7.506002	132.6	3.4	348.2	201.9	4
59	5.633179	7.506002	132.8	3.1	346.9	202.1	1.4
60	5.661499	7.506002	131.5	7.6	371.5	207.1	2
61	5.689819	7.506002	129.4	29.4	393.5	211.8	2.2
62	5.71814	7.506002	128.2	28.8	398.7	213.3	4.7
63	5.74646	7.506002	127.8	18.9	415.2	212.4	7.5
64	5.77478	7.506002	127.6	20.8	473.4	206.9	18.6
65	5.803101	7.506002	126.3	21.4	464.9	200	8.9
66	5.831421	7.506002	124	18	415.9	196.5	1.6
67	5.859741	7.506002	121.7	18	401.5	200.3	0.6

(*continued on next page*)

Table 4 (*continued*)

Fishnet no	Longitude	Latitude	R	LU	BT	Re	S
68	5.888062	7.506002	121.6	19.4	379.1	203.7	1.7
69	5.916382	7.506002	122.7	3.8	345.7	205.9	2.1
70	5.604858	7.543681	131.6	3.8	350.3	200.8	1.9
71	5.633179	7.543681	131.5	3.3	349.6	200.4	3.4
72	5.661499	7.543681	130.6	25.8	388.4	204.4	2.2
73	5.689819	7.543681	129.5	27.4	427.3	205	0.7
74	5.71814	7.543681	128.8	29.7	443.2	205.3	3.5
75	5.74646	7.543681	128.3	13.1	435	208.3	2.7
76	5.77478	7.543681	127.7	16.3	424.4	206.3	1
77	5.803101	7.543681	126.4	16.3	390.3	195.6	1.3
78	5.831421	7.543681	124.6	21.1	377.2	190.8	2.1
79	5.859741	7.543681	123.1	16.5	359.6	201	1.4
80	5.888062	7.543681	122.7	15.6	354	209	2.4
81	5.916382	7.543681	123	16	345.1	214.7	1.6
82	5.944702	7.543681	123.4	19	339.9	214.6	1
83	5.633179	7.58136	130.4	3.8	408.9	203.7	1.2
84	5.661499	7.58136	130.1	4	435.2	206.6	4.3
85	5.689819	7.58136	130	16.9	452.6	203.5	6
86	5.71814	7.58136	130.3	27.6	496.3	195	1.6
87	5.74646	7.58136	130.4	21	445.6	203.5	5.3
88	5.77478	7.58136	129.3	19.5	396.2	212.9	3.7
89	5.803101	7.58136	127	18.1	361.2	225.5	1.6
90	5.831421	7.58136	124.3	20.6	361.9	222.1	2
91	5.859741	7.58136	122.2	17.9	365.5	220.1	3.1
92	5.888062	7.58136	121.7	16.9	358.5	217.8	1.5
93	5.916382	7.58136	122.3	17.7	337	220.9	4.1
94	5.944702	7.58136	123.1	19	340.6	220.4	2.5
95	5.661499	7.619039	130	3.5	436.1	206.5	1.5
96	5.689819	7.619039	130.7	19.7	440.8	205.4	1.4
97	5.71814	7.619039	131.9	32.6	444.7	204.1	2.3
98	5.74646	7.619039	133.2	20.8	426.4	208.7	10.2
99	5.77478	7.619039	131.8	20.4	394.7	216.5	3.1
100	5.803101	7.619039	127.9	19.5	370.9	224.1	3
101	5.831421	7.619039	123.2	15.6	364.2	227.5	16.4
102	5.859741	7.619039	119.4	12.6	367.2	233	3
103	5.888062	7.619039	119.2	12.8	381.1	254.5	2.5
104	5.916382	7.619039	121.2	15.8	362.3	230.5	2.1
105	5.831421	7.656718	124.2	18.8	377	227.6	4
106	5.859741	7.656718	121.5	19.9	370.3	234.5	2.7
107	5.888062	7.656718	121.1	17	371.8	237.2	2.3
108	5.916382	7.656718	122.3	16.4	369.1	233.9	0.4
109	5.859741	7.694397	125.8	13.7	386.2	241.2	1
110	5.888062	7.694397	125.5	15.4	385.1	241.3	2.6
111	5.916382	7.694397	125.3	15.4	378.9	238.4	2.7
112	5.859741	7.732076	128.5	12.6	394.1	244.9	5.2
113	5.888062	7.732076	128.5	14.7	393	244.6	1

R: Rainfall; LU: Land use; BT: Bedrock topography; Re: Recharge rate; S; Slope.

$$C = \frac{d^-}{d^* + d^-} \tag{12}$$

3.3.3.3. Entropy weighting method. The object-oriented weighting method taken into consideration in this study is the entropy method, which is a crucial component of giving criteria used to rank alternatives' importance. The studies [16,38–40] used the entropy weighting technique for groundwater exploration and quality assessment. Results demonstrate noticeably high prediction accuracy. The method can be calculated as follows.

Assuming that a set of m fishnet points, (i = 1, 2, …, m) were extracted for the groundwater vulnerability assessment and that each point has n evaluating criteria, (j = 1, 2, …, n), is a reasonable assumption. Building a decision matrix (equ 13) is the first step in the computation process.

$$X = \left(X_{ij}\right)_{m\times n}(X_{11}\ X_{12}\ldots\ldots X_{1n}\ X_{2n}\ X_{2n}\ldots\ldots X_{2n}\ X_{m1}\ X_{m2}\ldots X_{mn}) \tag{13}$$

for $i = 1,2\ \ldots,m$; $j = 1,2,\ \ldots,n$

where X_{im} = feasible alternatives, X_{jn} = evaluation criteria, m = number of alternatives, n = number of criteria.

The matrix is then normalized by calculating the ratio of each criterion's value (X_{ij}) to the total of the criterion's arithmetic column sums. Equation (14) below displays the normalization equation for the matrix.

$$r_{ij} = \frac{x_{ij}}{\sum_{i=1}^{m} x_{ij}} \quad i = 1, 2...m;\ j = 1, 2, ...n \tag{14}$$

$$e_j = -h \sum_{i=1}^{m} r_{ij} \in r_{ij} \quad i = 1, 2...m;\ j = 1, 2, ...n \tag{15}$$

The entropy values (ej) is computed next with equations(15) and (16) where,

$$h = \frac{1}{m} \tag{16}$$

Finally, the entropy weight is computed using equ 17 below

$$w_j = \frac{1 - e_j}{n - \sum_{i=1}^{m} e_j} \tag{17}$$

where, $\sum_{j=1}^{n} w_j = 1$.

The relationship between the entropy weight and the values calculated for entropy at the penultimate stage is inverse. According to a study [19], the criterion with the higher weight provides more information and thus takes on a greater significance in the decision-making process.

3.3.3.4. Preparation of the Python-based TOPSIS, TOPSIS-entropy, and Entropy-WLA algorithms for the groundwater vulnerability assessment in the study area. The Python programming language was used to calculate the TOPSIS and TOPSIS-Entropy algorithm steps. The TOPSIS's outranking flow computation and the calculation of the weights were separated into two parts of the hybrid algorithm. Python classes were used to carry out the computations for weighting and ranking. The import of the required Python libraries, the assignment of values to variables, and the importation of the decision matrix's '.csv file' from the local machine all came before the declaration of these classes. The following are the codes for entropy weight computation:

```
df_ = pd.read_csv('Table 3.csv')
df = df_.drop(['Fishnet no', 'Longitude', 'Latitude'], axis=1)
fishnet_points = 114
conditioning_factors = 5
matrix = df.to_numpy()

class Entropy_weight:

    def __init__(self, conditioning_factors, fishnet_points):
        self.conditioning_factors = conditioning_factors
        self.fishnet_points = fishnet_points

    def en_weight(self, matrix):
        summation_x_ij = matrix.sum(axis=0)
        matrix_df = pd.DataFrame(matrix)

        for i in range(self.conditioning_factors):
            matrix_df[i] = matrix_df[i] / summation_x_ij[i]

        normalized_list = np.array(matrix_df)
        normalized_df = pd.DataFrame(normalized_list, columns=
                                ['R', 'LU', 'BT', 'Re', 'S'])

        h = 1 / np.log(self.fishnet_points)
        log_df = np.log(pd.DataFrame(normalized_df))

        entropy_data = normalized_df.mul(log_df)
        entropy_j = -h * entropy_data.sum(axis = 0)

        dj = 1 - entropy_j
        dj_sum = dj.sum(axis=0)

        en_weight =  dj/dj_sum

        return en_weight


Entropy = Entropy_weight(conditioning_factors, fishnet_points)
weight = np.array(Entropy.en_weight(matrix))
types = np.array([-1, -1, 1, -1, 1])

class TOPSIS:

    def __init__(self, conditioning_factors, fishnet_points,
                 weight, types):
        self.conditioning_factors = conditioning_factors
        self.fishnet_points = fishnet_points
        self.weight = weight
        self.types = types

    def closeness_coefficient(self, matrix):
        matrix_ = pd.DataFrame(matrix)
        squared_df = pd.DataFrame(matrix_) ** 2
        summation_x_ij = squared_df.sum(axis=0)

        for i in range(self.conditioning_factors):
```

1

```
        matrix_[i] = matrix_[i] / ((summation_x_ij[i]) ** 0.5)

    for i in range(self.conditioning_factors):
        matrix_[i] = matrix_[i] * weight[i]

    ideal_best = []
    ideal_worst = []
    positive_euc_dis = []
    negative_euc_dis = []
    positive_euc_df = matrix_.copy()
    negative_euc_df = matrix_.copy()

    for i in range(len(self.types)):
        if self.types[i] == -1:
            a = matrix_[i].min()
            ideal_best.append(a)
            b = matrix_[i].max()
            ideal_worst.append(b)
        else:
            a = matrix_[i].max()
            ideal_best.append(a)
            b = matrix_[i].min()
            ideal_worst.append(b)

    for i in range(self.fishnet_points):
        positive_euc_df.iloc[i] = (positive_euc_df.iloc[i]
        - ideal_best) ** 2
        negative_euc_df.iloc[i] = (negative_euc_df.iloc[i]
        - ideal_worst) ** 2

    for i in range(self.fishnet_points):
        a = (positive_euc_df.iloc[i].sum()) ** 0.5
        positive_euc_dis.append(a)
        b = (negative_euc_df.iloc[i].sum()) ** 0.5
        negative_euc_dis.append(b)

    summed_euc_dis = (np.array(positive_euc_dis)
                      + np.array(negative_euc_dis))
    closeness_coef = np.array(negative_euc_dis) / summed_euc_dis

    return pd.DataFrame(closeness_coef, columns = ['Cc'])
```

. (*continued*).

The computed entropy weights of the conditioning factors are shown in Table 4.

In addition, five groundwater vulnerability conditioning factors—rainfall (R), land use (LU), bedrock topography (BT), recharge rate (Re), and slope (S)—were taken into account in order to use the aforementioned codes. These factors are listed in Table 4 and served as inputs in the aforementioned algorithm. Furthermore, the type of the conditioning factors (beneficial or not), the number of fishnet points taken into account, the number of conditioning factors, as well as the weights that were computed using the Entropy_weight class, were all declared (Table 5). The TOPSIS-Entropy hybrid algorithm's first phase was the weightage calculation, and it was passed as an input in the second phased TOPSIS class along with the other crucial inputs mentioned earlier (see Table 6).

The Entropy-WLA model algorithm was also used to calculate the study area's groundwater vulnerability index. This model algorithm was applied to the conditioning factors that were used to evaluate each factor's impact on the study area's groundwater

Table 5
Calculated weights for Groundwater Vulnerability Conditioning Factors using python-based Entropy method.

	R	LU	BT	Re	S
Entropy values (e_j)	0.999933	0.983902	0.996257	0.999673	0.926869
d_j (1 - e_j)	0.000067	0.016098	0.003743	0.000327	0.073131
Entropy weights (w_j)	**0.000714**	**0.172419**	**0.040092**	**0.003498**	**0.783278**

R: Rainfall, **LU:** Land Use, **BT**: Bedrock Topography, **Re**: Recharge rate, **S**: Slope percent.

Table 6
Entropy weight, ratings and classification of the Groundwater Vulnerability Conditioning Factors (GVCF) produced thematic layers.

GVCF thematic layers	Category (classes)	Potential of groundwater vulnerability	Rating (R)	Entropy-Normalized weights (W)
Rainfall	118.7–122.2	Very low	5	0.000714
	122.2–124.9	Low	4	
	124.9–127.3	Medium	3	
	127.3–129.6	Medium-high	2	
	129.6–133.3	High	1	
Land Use	Vegetation	High	1	0.172419
	Water body	Medium-high	2	
	Built-up	Medium	3	
	Bare land	Low	4	
	Rock	Very low	5	
Bedrock topography	193.8–262.2	Very low	5	0.040092
	262.2–329.3	Low	4	
	329.3–395.0	Medium	3	
	395.0–460.7	Medium-high	2	
	460.7–542.8	High	1	
Recharge rate	176.29–202.64	Very low	5	0.003498
	202.64–210.39	Low	4	
	210.39–219.69	Medium	3	
	219.69–232.09	Medium-high	2	
	232.09–255.35	High	1	
Slope	0–2	High	1	0.783278
	2–8	Medium-high	2	
	8–15	Medium	3	
	15–30	Low	4	
	30–60	Very low	5	

vulnerability. Equation (18) below is the computing equation.

$$GVI = R_wR_r + LU_wLU_r + BT_wBT_r + Re_wRe_r + S_wS_r \quad (18)$$

where w is the normalized entropy weight of each conditioning factor and r is the ratings attached to each thematic layer of the factors considered.

Table 5 shows the details of the classes, ratings, and the entropy weight of each conditioning factor.

4. Results and discussion

4.1. Discussion of the derived vulnerability conditioning factors

4.1.1. Rainfall

The annual average volume of water that permeates the vadose zone and reaches the water table is referred to as rainfall (R). When assessing the groundwater vulnerability of an area, it's crucial to take the significance of the amount of rainfall into account. The study area's rainfall variation ranges from 118 to 134 mm/year, and this range was used to create the study area's rainfall map (Fig. 3a). The vulnerability of an area increases with the amount of rainfall there. The study area's spatial variation in average rainfall is classified into five categories: very low, low, medium, medium-high, and high. The area covered by each category is 148.12, 293.51, 290.67, 463.49, and 266.76 km^2, respectively. Towns in the study area like Irun and Ogbagi in the northwestern portion exhibit high average rainfall amounts, whereas Ora ojora, Ikeram, and Erushu in the north-eastern portion exhibit very low average rainfall amounts.

4.1.2. Land use

According to Olabode [23], land use (LU) refers to hydrogeological characteristics that influence an area's rate of infiltration, runoff, and evapotranspiration. The land use, which includes built-up areas, rocky areas, vegetation, bare land, and water bodies, greatly influences an aquifer unit's vulnerability. According to the Land Use/Land Cover map in Fig. 3b, the study area's land use is spatially distributed into five zones: built-up, rock, water body, vegetation, and bareland. The area of each of these zones is, respectively, 46.84, 370.86, 16.47, 490.25, and 568.13 km^2.

4.1.3. Bedrock topography

The quantitatively interpreted primary geoelectric parameters were used to determine the bedrock topography (BT). The bedrock's topography largely regulates surface water infiltration into the subsurface as groundwater flows from a high basement elevation to a lower basement elevation [41]. The study area's bedrock topography, which ranges from 190 to 554 m (Table 4), is characterized by depressions and ridges (low bedrock topography). The depression zones are located in the southern region, primarily in the Ose local government. Low runoff is present in depression zones, where it frequently allows more floodwater to percolate and contaminate the aquifer beneath, resulting in lowered groundwater quality. However, the evidence of high subsurface runoff rates is more pronounced within zones of ridges, which reduces contaminant infiltration to the underlain aquifer units and makes them less susceptible (more

protected). The depression zones cover an area of about 507.35 km^2, most of which is in Ose and all the other towns in the study area's southeastern and southwestern regions. Other areas, particularly in Akoko's northwest and northeast, are primarily covered by medium-to high-bedrock topography and include towns like Efifa, Ora-ojora, Ikeram, Ibarram, Arigidi, Auga (North), Ikare-akoko, Akungba, and Ukpe.

4.1.4. Recharge rate

The amount of water per unit area that permeates the subsurface through ponded infiltration or terrestrial infiltration and reaches the aquifer unit is referred to as the recharge rate (Re) of an aquifer unit [42]. The more quickly an aquifer unit recharges, the more vulnerable it becomes. This is primarily because an aquifer unit's rate of recharge significantly improves pollution and leachate flow

Table 7
Computed closeness coefficient (Cc) model results from the python-based TOPSIS-Entropy, TOPSIS and Entropy-WLA algorithms.

Fishnet no	TOPSIS-Entropy Cc	TOPSIS Cc	Entropy-WLA CC	Fishnet no	TOPSIS-Entropy Cc	TOPSIS Cc	Entropy-WLA CC
0	0.124556	0.149913	1.947145	57	0.267775	0.41492	2.389858
1	0.147435	0.207064	2.643817	58	0.157124	0.504093	2.567131
2	0.44494	0.289263	3.251178	59	0.084824	0.482709	1.783853
3	0.441602	0.307551	2.738133	60	0.091366	0.47118	1.780355
4	0.26128	0.271494	2.47561	61	0.074657	0.335906	1.871173
5	0.130547	0.248675	2.427808	62	0.1676	0.361262	2.348338
6	0.132914	0.208959	1.950643	63	0.275049	0.474668	2.348338
7	0.152179	0.224282	1.951357	64	0.691823	0.652058	3.8783
8	0.36636	0.285194	2.694543	65	0.326915	0.525703	2.581977
9	0.190015	0.254814	1.951357	66	0.066114	0.441279	1.056227
10	0.208113	0.272166	1.911265	67	0.045605	0.418849	1.574198
11	0.434129	0.309298	2.734635	68	0.067042	0.396176	1.783211
12	0.427404	0.337148	2.695257	69	0.099337	0.480834	2.393356
13	0.352432	0.34998	3.216012	70	0.094396	0.485843	1.783853
14	0.039918	0.259354	1.132913	71	0.137729	0.501325	2.567131
15	0.084081	0.305631	1.919689	72	0.077002	0.36304	2.567131
16	0.039342	0.267744	1.641746	73	0.029376	0.376662	1.051301
17	0.079391	0.307769	1.911265	74	0.122567	0.397325	1.834579
18	0.116401	0.23594	2.425024	75	0.105419	0.483598	2.351836
19	0.096245	0.2044	1.907767	76	0.054674	0.442659	1.396139
20	0.159726	0.2382	2.080186	77	0.060855	0.432754	1.612862
21	0.074175	0.228658	1.907767	78	0.077676	0.403847	2.569273
22	0.057148	0.229549	1.128701	79	0.06287	0.403808	1.613576
23	0.28427	0.305071	1.911979	80	0.093042	0.403981	2.565775
24	0.195147	0.311977	2.429236	81	0.068746	0.380986	1.60658
25	0.374734	0.350504	2.699469	82	0.049662	0.348678	1.778999
26	0.069302	0.285699	1.650884	83	0.080229	0.510652	1.740263
27	0.047701	0.239828	1.641746	84	0.166763	0.552708	2.523541
28	0.086976	0.219508	1.907767	85	0.219979	0.510498	2.523541
29	0.153063	0.245272	2.597443	86	0.055249	0.44547	1.013993
30	0.273507	0.306255	1.907767	87	0.192513	0.469972	1.833865
31	0.653212	0.482813	3.951488	88	0.134619	0.413719	1.831081
32	0.129295	0.340493	1.871887	89	0.065835	0.363093	1.602368
33	0.214046	0.363523	2.389144	90	0.074903	0.350343	1.603082
34	0.133794	0.349995	2.389144	91	0.114428	0.386552	2.38636
35	0.048707	0.313051	1.645958	92	0.06482	0.379391	1.776215
36	0.073329	0.332003	1.646672	93	0.150018	0.372608	2.38636
37	0.214788	0.361842	2.434162	94	0.092929	0.351652	2.38636
38	0.034318	0.26198	1.296908	95	0.086244	0.527524	1.740263
39	0.075226	0.288965	1.907767	96	0.058353	0.437011	1.740263
40	0.056174	0.37343	1.091393	97	0.076996	0.378319	1.833865
41	0.196329	0.441139	2.351836	98	0.375859	0.506669	3.306819
42	0.242379	0.469979	2.484877	99	0.11263	0.39592	2.560135
43	0.219708	0.3773	2.521471	100	0.109729	0.372143	1.867675
44	0.394251	0.490367	2.618571	101	0.610059	0.553543	3.952916
45	0.289971	0.445127	2.047804	102	0.115598	0.416234	1.866319
46	0.077203	0.309336	2.389858	103	0.099286	0.403791	2.555995
47	0.040121	0.334759	1.65017	104	0.083447	0.381573	2.559493
48	0.128472	0.408394	2.436946	105	0.145815	0.387892	2.38636
49	0.105775	0.338561	1.871173	106	0.098998	0.354547	2.383576
50	0.16139	0.341784	1.871173	107	0.088382	0.374306	2.383576
51	0.045042	0.365054	1.087895	108	0.047226	0.367005	1.599584
52	0.94378	0.644261	3.361043	109	0.059197	0.398981	1.771289
53	0.043579	0.498323	1.360259	110	0.09976	0.396706	2.554567
54	0.262099	0.490583	2.313172	111	0.103034	0.395057	2.382148
55	0.073052	0.410888	1.569986	112	0.19262	0.445542	2.553853
56	0.189332	0.403196	2.393356	113	0.05742	0.393806	1.598156

movement. The study area's recharge rate ranges from 176 to 256 mm/year based on the values in Table 4. The very low, low, medium, medium-high, and high zones of the study area, with area extents of 205.96, 475.37, 408.4, 264.9, and 137.92 km^2, respectively, are depicted on the thematic map, Fig. 4a, of Re, which was generated. The map that was created reveals that the majority of Akoko's north-eastern region has a medium to high rate of recharge, indicating that this area is extremely vulnerable to surface-level pollution. Towns in Akoko's southwest and Ose (which include Oba, Ikun, and Afo) are also highly vulnerable to this type of pollution. However, those towns viz: Iru, Ogbagi, and Igbe (northwest) Odowara, Oka akoko, Imeri, Idogun, Ipesi, Idosale, Ekpemi (southwest, central and

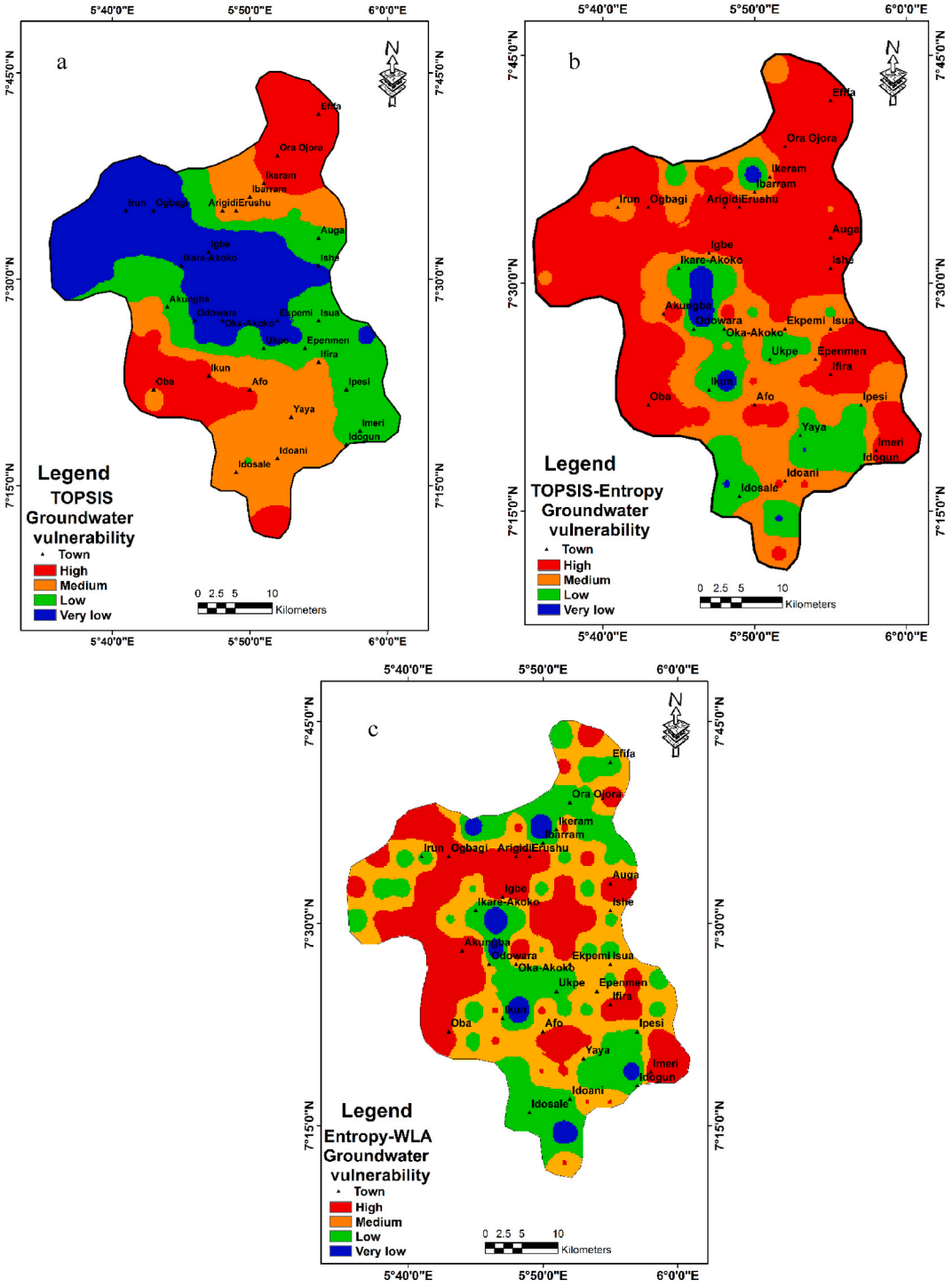

Fig. 6. The Groundwater vulnerability model maps of the study area based on.

southeast) which fall within the low and very low zones will be characterized by low vulnerability potentiality [43].

4.1.5. Slope

The ASTER GLOBAL DEM image was used to create the slope map (Fig. 1e). According to Table 4's soil terrain model (European Commission, 1995), the map was divided into five different slope classes. The five classes identified are 0–2, 2–8, 8–15, 15–30, and 30–60, which correspond to classifications for flat, undulating, rolling, moderately steep, and steep terrain, respectively. The study area is primarily distinguished by its flat to undulating slope (84%), low runoff, and high infiltration rates. Low-sloped areas frequently have long-lasting water retention. This encourages contaminant migration and water recharge infiltration. As a result, it appears from the study area's slope map that the majority of the groundwater there is relatively susceptible to contamination.

4.2. The TOPSIS, Entropy-WLA, and TOPSIS-entropy models application results and groundwater vulnerability model map of the study area

The goal of this study is to investigate the effectiveness of object-oriented data mining techniques in groundwater vulnerability assessment in a complex geologic environment and to compare their performance to other algorithms that have been taken into consideration. This goal is illustrated by the methodology flowchart in Fig. 2. The steps of application were used to compute the vulnerability indices using the TOPSIS, Entropy-WLA, and TOPSIS-Entropy model algorithms, as shown in Fig. 2. The first step of computation for the TOPSIS and TOPSIS-Entropy algorithms in this study entails the construction of fishnet points on each thematic layer of the conditioning factors and the extraction of pixel values (Table 4). This table, along with additional parameters, was used as an input for the Python-based TOPSIS and TOPSIS-Entropy model algorithms, as was previously mentioned. Both algorithms return the computed closeness coefficient (Cc), which displays the ranking variation of the vulnerability index in the research area. Using the following codes, the calculated Cc was output.

```
Topsis = TOPSIS(conditioning_factors, fishnet_points, weight, types)
Topsis.closeness_coefficient(matrix)
```

Using the inverse distance weighted (IDW) interpolation technique of the ArcGIS software, the computed vulnerability indexes (Table 7) were used to create the TOPSIS and TOPSIS-Entropy groundwater vulnerability model maps (Fig. 6a and b) of the study area. Additionally, Table 7 entry for the Entropy-WLA algorithm index computed using equation (18) was used to create the study area's Entropy-WLA based groundwater vulnerability map. The maps that resulted were divided into four vulnerability classes using the Natural Breaks Approach [44], as shown in Fig. 6a, b, and c.

The study area's groundwater vulnerability index spatial variation is divided into zones of high, medium, low, and very low vulnerability. The majority of the study area is occupied by the medium to high regions (Table 8), which have coverage rates of 45 and 82% for the TOPSIS and TOPSIS-Entropy model maps, respectively, and 73% for the Entropy-WLA model map. The remaining portion is covered by regions with very low to low groundwater vulnerability.

4.2.1. Validation of model result

The geoelectrically derived longitudinal conductance parameter was used as the aquifer protective capacity indicator in a correlation approach technique for the validation of the produced groundwater vulnerability model maps. This technique was used to assess the performance of the reliability of their environmental decision-making. This method is consistent with the study [45] which reported that the longitudinal conductance of an area provides a good understanding of the area's ability to protect its aquifer. The longitudinal conductance map in Fig. 7 was created for visual inspection correlation with Fig. 6(a,b,c) using the computed longitudinal conductance (Lc) parameter result in Table 3. Nonetheless, the analysis for the quantitative correlation (Table 9) in determining success rate is as follows:

For the TOPSIS-Entropy prediction model map:

Total number of fishnet observation points = 114
Number of fishnets where the expected and the actual longitudinal conductance classifications coincide = 80.
Number of fishnets where the expected and the actual longitudinal conductance classifications did not coincide = 34.

Table 8
The Areal characteristics of the groundwater vulnerability model maps.

Groundwater vulnerability classification	TOPSIS		TOPSIS-Entropy		Entropy-WLA	
	Areal Extent (Km^2)	Percentage Coverage (%)	Areal Extent (Km^2)	Percentage Coverage (%)	Areal Extent (Km^2)	Percentage Coverage (%)
High	279	19	798.25	54	567.169	38
Medium	397	26	419	28	522.3925	35
Low	358	24	240.3	16	343.2865	23
Very low	458.55	31	35	2	59.702	4

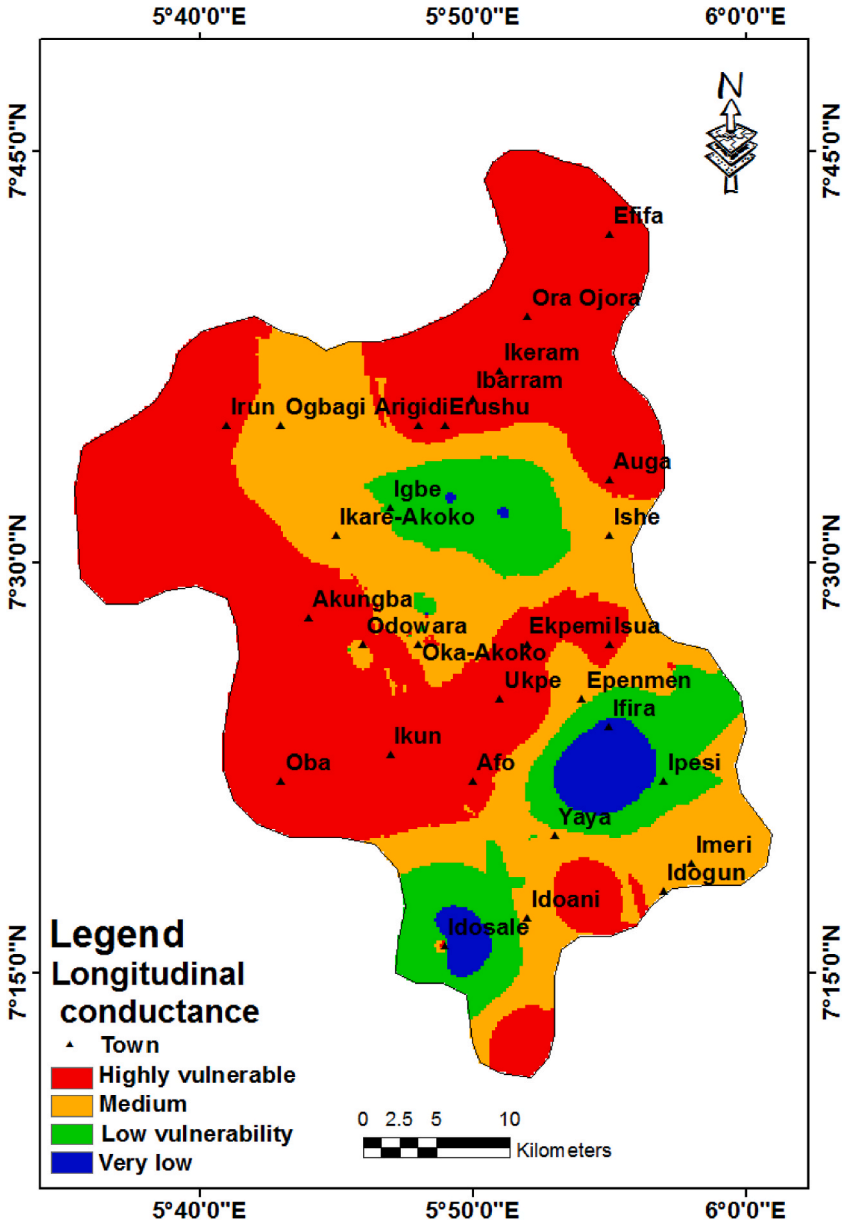

Fig. 7. Longitudinal conductance map of the study area.

Success rate (accuracy) of the prediction $= \frac{80}{114} \times 100 = 70\%$.

Similarly, for the TOPSIS prediction model map, it is as follows:

Number of fishnets where the expected and the actual longitudinal conductance classifications coincide = 57.
Number of fishnets where the expected and the actual longitudinal conductance classifications did not coincide = 57.
Success rate (accuracy) of the prediction $= \frac{57}{114} \times 100 = 50\%$.

Similarly, for the Entropy-WLA prediction model map, it is as follows:

Number of fishnets where the expected and the actual longitudinal conductance classifications coincide = 54.
Number of fishnets where the expected and the actual longitudinal conductance classifications did not coincide = 60.
Success rate (accuracy) of the prediction $= \frac{54}{114} \times 100 = 47\%$.

Table 9
Validation results for the groundwater vulnerability model maps.

Fishnet no	Lc (m/ρ)	Lc description	Entropy-WLA model map vulnerability description	Remark	TOPSIS model map vulnerability description	Remark	Expected vulnerability description from TOPSIS-Entropy model map	Remark
0	0.003657	Very low - Low	Very low	Coincide	Very low	Coincide	High	Not coincide
1	0.039463	Medium - High	Low	Not coincide	Low	Not coincide	Low	Not coincide
2	0.024908	Very low - Low	High	Not coincide	Low	Coincide	Very Low	Coincide
3	0.039788	Medium - High	High	Coincide	Low	Not coincide	Low	Not coincide
4	0.049858	Medium - High	Medium	Coincide	Medium	Coincide	Low	Not coincide
5	0.027896	Medium - High	Very low	Not coincide	Low	Not coincide	Low	Not coincide
6	0.014202	Very low - Low	Very low	Coincide	Low	Coincide	High	Not coincide
7	0.010855	Very low - Low	Low	Coincide	Low	Coincide	High	Not coincide
8	0.024918	Very low - Low	Medium	Not coincide	Low	Coincide	Low	Coincide
9	0.025353	Very low - Low	Low	Coincide	Low	Coincide	High	Not coincide
10	0.025485	Very low - Low	Low	Coincide	Low	Coincide	High	Not coincide
11	0.015288	Very low - Low	Medium	Not coincide	Low	Coincide	Low	Coincide
12	0.01546	Very low - Low	Medium	Not coincide	Low	Coincide	Low	Coincide
13	0.019287	Very low - Low	Medium	Not coincide	Medium	Not coincide	Very Low	Coincide
14	0.019614	Very low - Low	Very low	Coincide	Medium	Not coincide	High	Not coincide
15	0.021107	Very low - Low	Very low	Coincide	Medium	Not coincide	High	Not coincide
16	0.005815	Very low - Low	Very low	Coincide	Very low	Coincide	High	Not coincide
17	0.00842	Very low - Low	Very low	Coincide	Low	Coincide	High	Not coincide
18	0.006303	Very low - Low	Very low	Coincide	Very low	Coincide	Low	Coincide
19	0.006149	Very low - Low	Very low	Coincide	Very low	Coincide	High	Not coincide
20	0.009504	Very low - Low	Low	Coincide	Very low	Coincide	Medium	Not coincide
21	0.010638	Very low - Low	Very low	Coincide	Very low	Coincide	High	Not coincide
22	0.02125	Very low - Low	Very low	Coincide	Low	Coincide	High	Not coincide
23	0.043158	Medium - High	Medium	Coincide	Low	Not Coincide	High	Coincide
24	0.054886	Medium - High	Low	Not coincide	Low	Not coincide	Low	Not coincide
25	0.033977	Medium - High	Medium	Coincide	Medium	Coincide	Low	Not coincide
26	0.025293	Very low - Low	Very low	Coincide	Medium	Not Coincide	High	Not coincide
27	0.006013	Very low - Low	Very low	Coincide	Very low	Coincide	High	Not coincide
28	0.005916	Very low - Low	Very low	Coincide	Very low	Coincide	High	Not coincide
29	0.006435	Very low - Low	Low	Coincide	Very low	Coincide	Low	Coincide
30	0.007417	Very low - Low	Medium	Not Coincide	Very low	Coincide	High	Not coincide
31	0.006595	Very low - Low	High	Not Coincide	Low	Coincide	Very Low	Coincide
32	0.006128	Very low - Low	Low	Not coincide	Low	Coincide	High	Not coincide

(*continued on next page*)

Table 9 (*continued*)

Fishnet no	Lc (m/ρ)	Lc description	Entropy-WLA model map vulnerability description	Remark	TOPSIS model map vulnerability description	Remark	Expected vulnerability description from TOPSIS-Entropy model map	Remark
33	0.010345	Very low - Low	Low	Coincide	Low	Coincide	Low	Coincide
34	0.033017	Medium - High	Low	Coincide	Medium	Coincide	Low	Not coincide
35	0.048467	Medium - High	Very low	Not Coincide	Low	Not coincide	High	Coincide
36	0.03943	Medium - High	Very low	Not Coincide	Medium	Coincide	High	Coincide
37	0.031298	Medium - High	Low	Not coincide	Medium	Coincide	Low	Not coincide
38	0.006008	Very low - Low	Very low	Coincide	Very low	Coincide	High	Not coincide
39	0.006103	Very low - Low	Very low	Coincide	Very low	Coincide	High	Not coincide
40	0.009887	Very low - Low	Very low	Coincide	Medium	Not Coincide	High	Not coincide
41	0.012102	Very low - Low	Low	Coincide	High	Not Coincide	Low	Coincide
42	0.013824	Very low - Low	Low	Coincide	High	Not Coincide	Low	Coincide
43	0.010162	Very low - Low	Low	Coincide	Medium	Not Coincide	Low	Coincide
44	0.00832	Very low - Low	Medium	Not Coincide	High	Not Coincide	Low	Coincide
45	0.015935	Very low - Low	Medium	Not Coincide	High	Not Coincide	Medium	Not coincide
46	0.020526	Very low - Low	Very low	Coincide	Medium	Not Coincide	Low	Coincide
47	0.022236	Very low - Low	Very low	Coincide	Medium	Not Coincide	High	Not coincide
48	0.026705	Medium - High	Low	Not coincide	High	Coincide	Low	Not coincide
49	0.006285	Very low - Low	Very low	Coincide	Low	Coincide	High	Not coincide
50	0.006826	Very low - Low	Low	Coincide	Low	Coincide	High	Not coincide
51	0.010011	Very low - Low	Very low	Coincide	Medium	Not Coincide	High	Not coincide
52	0.015653	Very low - Low	High	Not Coincide	High	Not Coincide	Very Low	Coincide
53	0.036469	Medium - High	Very low	Not coincide	High	Coincide	High	Coincide
54	0.022029	Very low - Low	Medium	Not coincide	High	Not Coincide	Low	Coincide
55	0.01139	Very low - Low	Very low	Coincide	High	Not Coincide	High	Not coincide
56	0.011841	Very low - Low	Low	Coincide	Medium	Not Coincide	Low	Coincide
57	0.010033	Very low - Low	Medium	Not Coincide	Medium	Not Coincide	Low	Coincide
58	0.010613	Very low - Low	Low	Coincide	High	Not Coincide	Low	Coincide
59	0.010703	Very low - Low	Low	Coincide	High	Not Coincide	High	Not coincide
60	0.009362	Very low - Low	Low	Coincide	High	Not Coincide	High	Not coincide
61	0.010061	Very low - Low	Very low	Coincide	Medium	Not Coincide	High	Not coincide
62	0.012442	Very low - Low	Low	Coincide	Medium	Not Coincide	Low	Coincide
63	0.017854	Very low - Low	Medium	Not Coincide	Medium	Not Coincide	Low	Coincide
64	0.022411	Very low - Low	High	Not Coincide	High	Not Coincide	Very Low	Coincide
65	0.024605	Very low - Low	Medium	Not Coincide	High	Not Coincide	Low	Coincide

(*continued on next page*)

Table 9 (*continued*)

Fishnet no	Lc (m/ρ)	Lc description	Entropy-WLA model map vulnerability description	Remark	TOPSIS model map vulnerability description	Remark	Expected vulnerability description from TOPSIS-Entropy model map	Remark
66	0.02669	Medium - High	Very low	Not Coincide	High	Coincide	High	Coincide
67	0.031576	Medium - High	Very low	Not Coincide	High	Coincide	High	Coincide
68	0.027017	Medium - High	Very low	Not Coincide	High	Coincide	High	Coincide
69	0.019463	Very low - Low	Low	Coincide	High	Not Coincide	Low	Coincide
70	0.01077	Very low - Low	Low	Coincide	High	Not Coincide	High	Not coincide
71	0.010903	Very low - Low	Low	Coincide	High	Not Coincide	Low	Coincide
72	0.011107	Very low - Low	Very low	Coincide	High	Not Coincide	Low	Coincide
73	0.01368	Very low - Low	Very low	Coincide	High	Not Coincide	High	Not coincide
74	0.01794	Very low - Low	Very low	Coincide	High	Not Coincide	High	Not coincide
75	0.022703	Very low - Low	Low	Coincide	High	Not Coincide	Low	Coincide
76	0.027369	Medium - High	Very low	Not coincide	High	Coincide	High	Coincide
77	0.034677	Medium - High	Very low	Not Coincide	High	Not Coincide	High	Coincide
78	0.037923	Medium - High	Very low	Not Coincide	High	Not Coincide	Low	Not coincide
79	0.03494	Medium - High	Very low	Not Coincide	High	Not Coincide	High	Coincide
80	0.023822	Very low - Low	Low	Coincide	Medium	Not Coincide	Low	Coincide
81	0.014139	Very low - Low	Very low	Coincide	Medium	Not Coincide	High	Not coincide
82	0.013297	Very low - Low	Very low	Coincide	Medium	Not Coincide	High	Not coincide
83	0.008925	Very low - Low	Low	Coincide	High	Not Coincide	High	Not coincide
84	0.006193	Very low - Low	Low	Coincide	High	Not Coincide	Low	Coincide
85	0.012029	Very low - Low	Low	Coincide	High	Not Coincide	Low	Coincide
86	0.022315	Very low - Low	Very low	Coincide	High	Not Coincide	High	Not coincide
87	0.019692	Very low - Low	Low	Coincide	High	Not Coincide	High	Not coincide
88	0.015413	Very low - Low	Low	Coincide	Medium	Not Coincide	High	Not coincide
89	0.004515	Very low - Low	Very low	Coincide	Low	Coincide	High	Not coincide
90	0.011445	Very low - Low	Very low	Coincide	Low	Coincide	High	Not coincide
91	0.015141	Very low - Low	Low	Coincide	Low	Coincide	Low	Coincide
92	0.013145	Very low - Low	Very low	Coincide	Medium	Not Coincide	High	Not coincide
93	0.005604	Very low - Low	Low	Coincide	Low	Coincide	Low	Coincide
94	0.008909	Very low - Low	Very low	Coincide	Low	Coincide	Low	Coincide
95	0.008401	Very low - Low	Low	Coincide	High	Not Coincide	High	Not coincide
96	0.010786	Very low - Low	Very low	Coincide	High	Not Coincide	High	Not coincide
97	0.016132	Very low - Low	Very low	Coincide	High	Not Coincide	High	Not coincide
98	0.016567	Very low - Low	Medium	Not Coincide	High	Not Coincide	Very Low	Coincide

(*continued on next page*)

Table 9 (*continued*)

Fishnet no	Lc (m/ρ)	Lc description	Entropy-WLA model map vulnerability description	Remark	TOPSIS model map vulnerability description	Remark	Expected vulnerability description from TOPSIS-Entropy model map	Remark
99	0.013025	Very low - Low	Low	Coincide	Medium	Not Coincide	Low	Coincide
100	0.008907	Very low - Low	Low	Coincide	Low	Coincide	High	Not coincide
101	0.007285	Very low - Low	High	Not coincide	Low	Coincide	Very Low	Coincide
102	0.006238	Very low - Low	Low	Coincide	Very low	Coincide	High	Not coincide
103	0.000531	Very low - Low	Low	Coincide	Very low	Coincide	Low	Coincide
104	0.006588	Very low - Low	Low	Coincide	Very low	Coincide	Low	Coincide
105	0.009818	Very low - Low	Low	Coincide	Low	Coincide	Low	Coincide
106	0.007971	Very low - Low	Very low	Coincide	Very low	Coincide	Low	Coincide
107	0.006799	Very low - Low	Medium	Not Coincide	Very low	Coincide	Low	Coincide
108	0.007609	Very low - Low	Very low	Coincide	Very low	Coincide	High	Not coincide
109	0.005123	Very low - Low	Very low	Coincide	Very low	Coincide	High	Not coincide
110	0.005314	Very low - Low	Low	Coincide	Very low	Coincide	Low	Coincide
111	0.007452	Very low - Low	Low	Coincide	Very low	Coincide	Low	Coincide
112	0.001251	Very low - Low	Low	Coincide	Very low	Coincide	Low	Coincide
113	0.002078	Very low - Low	Very low	Coincide	Very low	Coincide	High	Not coincide

According to the aforementioned correlation findings, the estimated groundwater vulnerability values generated by the proposed TOPSIS-entropy based model are the best index predictor variable for explaining the response variable, which is the area's longitudinal conductance. By way of comparison, this performance outperforms that of the other predictive models applied in this study. Accordingly, the developed groundwater vulnerability model map based on surface and subsurface data integrated results with the proposed TOPSIS-entropy-based model can be used with confidence for groundwater resources exploration and management in the study area.

Additionally, a qualitative analysis of the TOPSIS-Entropy model map reveals a strong correlation with each of the vulnerability conditioning parameters taken into consideration. The 'medium' and 'high' groundwater vulnerability classes that the model predicted are typical of regions with medium to high recharge rates, relatively high rainfall, and high bedrock topography. Additionally, these predicted zones are consistent with the study area's built-up, vegetated, and waterbody land use zones as well as zones with flat to undulating slopes.

5. Conclusion

In this study, the groundwater vulnerability assessment in a multifaceted geologic setting was carried out, this was demonstrated by employing the application of object-oriented multi-criteria decision methods (MCDM) to geophysical, climatic, and remote sensing parameters. 114 evenly spaced observation points were subjected to the object-oriented TOPSIS-Entropy MCDM algorithm across the study area's thematic layers that addressed groundwater vulnerability conditioning factors. These layers were created spatially by using GIS to process surface and subsurface (geophysical, climatic, and remote sensing) data. Python's computational power was used to reduce the cost of computing the model algorithm used in the study.

The hybrid TOPSIS-Entropy data mining technique was used to rank and weigh the conditioning factors. Utilizing the entropy method of weightage, the weights of the conditioning factors were calculated. This approach was used with the variables of rainfall (R), land use (LU), bedrock topography (BT), recharge rate (Re), and slope (S). The slope parameter had the highest weight when using the Python-based Entropy Class, while rainfall had the lowest weight. By calculating the closeness coefficient of each observation point to the ideal solution, the TOPSIS algorithm, which was programmed in Python, was used to rank the alternatives. The groundwater vulnerability model map of the study area was calculated using the closeness coefficient.

In comparison, the study area's groundwater vulnerability was ranked using the TOPSIS and Entropy-WLA based algorithms. The closeness coefficient index, which was computed using a subjective weight in the TOPSIS algorithm, was used to create the study area's TOPSIS-based groundwater vulnerability map. Additionally, to create the Entropy-WLA based groundwater vulnerability map of the study area, the weight linear algorithm was used to compute the vulnerability index.

The success rate technique was used to validate the generated models. When compared to the other models under consideration, TOPSIS and Entropy-WLA, which had success rates of 50% and 47%, respectively, the TOPSIS-Entropy based groundwater vulnerability model demonstrated commensurably higher success rates of 70%. The validation's findings indicate that the TOPSIS-Entropy (object-oriented) based groundwater vulnerability model performed best in terms of accuracy. When it comes to groundwater management and development in the study area, this developed model map can serve as a guide for decision-makers. Additionally, methods for model development can be investigated as a guide for the creation of models for other groundwater management domains in areas with comparable geology.

Author contribution statement

Olanrewaju Fred Atenidegbe: Conceived and designed the experiments; Performed the experiments; Analyzed and interpreted the data; Contributed reagents, materials, analysis tools or data; Wrote the paper.

Kehinde Anthony Mogaji: Conceived and designed the experiments; Contributed reagents, materials, analysis tools or data.

Data availability statement

Data will be made available on request.

Declaration of competing interest

The authors declare that they have no known competing financial interests or personal relationships that could have appeared to influence the work reported in this paper

[5]

References

[1] F.R. Gandhi, J.N. Patel, Groundwater potentiality deciphering and sensitivity study using remote sensing technique and fuzzy approach, Acta Geophys. 70 (2022) 265–282, https://doi.org/10.1007/s11600-021-00711-5.

[2] H.G. Rendilicha, P.G. Home, J.M. Raude, A preliminary review of Groundwater vulnerability assessment and pollution status in Kenya, Acque Sotterranee-italian Journal of Groundwater (2018), https://doi.org/10.7343/as-2018-328.

[3] I. Ouedraogo, P. Defourny, M. Vanclooster, Mapping the groundwater vulnerability for pollution at the pan African scale, Sci. Total Environ. 544 (2016) 939–953.

[4] O.J. Akintorinwa, M.O. Atitebi, A.A. Akinlalu, Hydrogeophysical and aquifer vulnerability zonation of a typical basement complex terrain: a case study of Ododе Idanre southwestern Nigeria, Heliyon 6 (2020), e04549.

[5] M. Sahoo, S. Sahoo, A. Dhar, B. Pradhan, Effectiveness Evaluation of objective and subjective weighting methods for aquifer vulnerability assessment in urban context, J. Hydrol. 541 (2016) 1303–1315, https://doi.org/10.1016/j.jhydrol.2016.08.035.

[6] K.A. Mogaji, Application of vulnerability modeling techniques in groundwater resources management: a comparative study, Appl. Water Sci. 8 (2018) 127, https://doi.org/10.1007/s13201-018-0770-2.

[7] L. Huang, G. Zeng, J. Liang, S. Hua, Y. Yuan, X. Li, H. Dong, J. Liu, S. Nie, J. Liu, Combined Impacts of Land use and climate change in the Modeling of future groundwater vulnerability, J. Hydrol. Eng. (2017), https://doi.org/10.1061/(ASCE)HE.1943-5584.0001493.

[8] O.O. Omotola, M.I. Oladapo, O.J. Akintorinwa, Modeling assessment of groundwater vulnerability to contamination risk in a typical basement terrain case of vulnerability techniques application comparison study, Model. Earth Syst. Environ. (2020), https://doi.org/10.1007/s40808-020-00720-1.

[9] D. Goyal, A.K. Haritash, S.K. Singh, A comprehensive review of groundwater vulnerability assessment using index-based, modeling, and coupling methods, J. Environ. Manag. (2022), https://doi.org/10.1016/j.jenvman.2021.113161.

[10] K.A. Mogaji, H.S. Lim, Development of groundwater favourability map using GIS-based driven data mining models: an approach for effective groundwater resource management, Geocarto Int. (2017), https://doi.org/10.1080/10106049.2016.1273400.

[11] N. Khodabakhshi, N. Heidarzadeh, G. Asadollahfardi, Vulnerability assessment of the Sefid-Dasht aquifer using a modified GIS based Fuzzy-DRASTIC method (in press), J. Am. Water Works Assoc. (2017), https://doi.org/10.5942/jawwa.2017.109.0039.

[12] A.A. Akinlalu, A. Adegbuyiro, K.A.N. Adiat, B.E. Akeredolu, W.Y. Lateef, Application of multi-criteria decision analysis in prediction of groundwater resources potential: a case of Oke-Ana, Ilesa area, southwestern, Nigeria, NRIAG J. Astron. Geophys. 6 (2017) 182–200.

[13] G.P. Panagopoulos, A.K. Antonakos, N.J. Lambrakis, Optimization of the DRASTIC method for groundwater vulnerability assessment via the use of simple statistical methods and GIS, Hydrol. J 14 (2006) 894–911.

[14] A.M. Al-Abadi, S. Shahid, Spatial mapping of artesian zone at Iraqi southern desert using a GIS-based random forest machine learning model, Model. Earth Syst. Environ. 2 (2016) 96.

[15] C.L. Hwang, K. Yoon, Multiple Attribute Decision Making Methods and Applications, Springer-Verlag, New York, Berlin, 1981, https://doi.org/10.1007/978-3-642-48318-9.

[16] P. Li, J. Wu, H. Qian, Groundwater quality assessment based on rough sets attribute reduction and TOPSIS method in a semi-arid area, China, Environ. Monit. Assess. 184 (2012) 4841–4854, https://doi.org/10.1007/s10661-011-2306-1.

[17] E. Minarčíková, Application of selected weighting methods and topsis method in regional disparities analysis, in: The 10th International Days of Statistics and Economics, Prague, September 8-10, 2016.

[18] E. Roszkowska, Application the TOPSIS methods for ordering offers in Buyer–seller transaction, Optim.– Studia Ekonomiczne 3 (43) (2009) 117–133.

[19] T.I. Ayşegül, A.A. Esra, The decision-making approach based on the combination of entropy and Rov methods for the Apple selection problem, Eur. J. Interdiscipl. Stud. 3 (3) (2017).

[20] Y. Qi, F. Wen, K. Wang, L. Li, S.N. Singh, A fuzzy comprehensive evaluation and entropy weight decision-making based method for power network structure assessment, Int. J. Eng. Sci. Technol. 2 (5) (2010) 92–99.

[21] R.K. Garg, R. Sharma, K. Sharma, MCDM based evaluation and ranking of commercial off-the-shelf using fuzzy based matrix method, Decis. Sci. Lett. 6 (2) (2017) 117–136.

[22] M. Butwall, P. Ranka, S. Shah, Python in Field of Data Science, 2019, https://doi.org/10.5120/ijca2019919404. A Review.

[23] O.F. Olabode, Potential groundwater recharge sites mapping in a typical basement terrain: a GIS methodology approach, J. Geovisualization Spatial Anal. (2019), https://doi.org/10.1007/s41651-019-0028-z.

[24] A.O. Eludoyin, T.A. Ojo, T. Ojo, O. Awotoye, Effects of artisanal gold mining activities on soil properties in a part of southwestern Nigeria, Cogent Environ. Sci. 3 (1) (2017), https://doi.org/10.1080/23311843.2017.1305650.
[25] J.O. Ajayi. Water from Rocks, an Inaugural Lecture Delivered at the Obafemi Awolowo University Press, Ile-Ife on 11th April, (2017). Inaugural lecture series press, Ile-ife 67pp.
[26] S. Diop, M.N. Tijani, Assessing the basement aquifer of Eastern Senegal, Hydrogeol. J. 26 (2008) 1349–1369.
[27] M.A. Rahaman, in: Geological Survey of Nigeria (Ed.), Recent Advances in the Study of the Basement Complex of Nigeria, Precambrian Geology Nigeria, 1988, pp. 11–43.
[28] Nigeria Geological Survey Agency (NGSA), Published by the Authority of the Federal Republic of Nigeria, 2006.
[29] L. Aller, T. Bennet, J.H. Lehr, R.J. Petty, DRASTIC: A Standardized System for Evaluating Ground Water Pollution Using Hydrogeologic Settings, vol. 600, EPA. U.S. Environmental Protection Agency, 1985, pp. 2–85.
[30] O.E. Aluko, O. Igwe, An integrated geomatics approach to groundwater potential delineation in the Akoko-Edo area, Nigeria, Environ. Earth Sci. 76 (2017) 240–244.
[31] O.O. Aladejana, A.Y.B. Anifowose, B.J. Fagbohun, Testing the ability of an empirical hydrological model to verify a knowledge-based groundwater potential zone mapping methodology, Model Earth Syst. Environ. 2 (174) (2016) 1–17.
[32] S.I. El-mahdy, M.M. Mohamed, Land-use/land cover change impact on groundwater quantity and quality: a case study of Ajman Emirate, the United Arab Emirate, using remote sensing and GIS, Arabian J. Geosci. 9 (2016) 722.
[33] B. Nas, A. Berktay, Groundwater quality mapping in urban groundwater using GIS, Environ. Monit. Assess. 160 (1–4) (2008) 215–227.
[34] M.H. Loke, Tutorial: 2-D and 3-D Electrical Imaging Surveys, 1999.
[35] B.P.A. Vander-Velper, WinRESIST Version 1.0 Resistivity Depth Sounding Interpretation Software M.Sc. Research Project, ITC, Delft Netherland, 2004.
[36] M.M.D. Widianta, T. Rizaldi, D.P.S. Setyohadi, H.Y. Riskiawan, Comparison of multi-criteria decision support methods (AHP, TOPSIS, SAW & PROMENTHEE) for employee placement, J. Phys.: Conf. Ser. 953 (2018), 012116.
[37] J. Kittur, Using PROMETHEE and TOPSIS multi-criteria decision making methods to evaluate optimal generation, in: International Conference on Power and Advanced Control Engineering, 2015, 978-1-4799-8371-1/15.
[38] A.M. Al-Abadi, H.R. Pourghasemi, S. Shahid, H.B. Ghalib, Spatial mapping of groundwater potential using entropy weighted linear aggregate Novel approach and GIS, Arabian J. Sci. Eng. 42 (2017) 1185–1199.
[39] A.M. Al-Abadi, S. Shahid, A comparison between index of entropy and catastrophe theory methods for mapping groundwater potential in an arid region, Environ. Monit. Assess. 187 (9) (2015) 4801.
[40] H. Safari, M.S. Fagheyi, S.S. Ahangari, M.R. Fathi, Applying Promethee method based on entropy weight for supplier selection, Bus. Manag. Strat. 3 (1) (2012) 97–106.
[41] A. Srivastava, Aquifer geometry, basement topography and groundwater quality around Ken graben, India, J. Spatial Hydrol. 2 (2) (2002).
[42] R. Anderson, M.-H. Lo, S. Swenson, J.S. Famiglietti, Q. Tang, T. Skaggs, Y.-H. Lin, R.-J. Wu, Using satellite-based estimates of evapotranspiration and groundwater changes to determine anthropogenic water fluxes in land surface models, Geosci. Model Dev. (GMD) 8 (10) (2015) 3021–3031, https://doi.org/10.5194/gmd-8-3021-2015.
[43] K.A. Mogaji, H.S. Lim, K. Abdullah, Modeling of groundwater recharge using a multiple linear regression (MLR) recharge model developed from geophysical parameters: a case of groundwater resources management, Environ. Earth Sci. 73 (2015) 1217–1230, https://doi.org/10.1007/s12665-014-3476-2.
[44] G.F. Jenks, 'The data model concept in statistical model identification' international yearbook of Cartography, vol 7, 1967, pp. 186–190.
[45] M.I. Oladapo, O.J. Akintorinwa, Hydrogeophysical study of Ogbese south western Nigeria, Global J. Pure Appl. Sci. 13 (1) (2007) 55–61.